AFOSR Final Scientific Report
AFOSR No. 70-1376 TR

Final Report on

Quenching of Solid Propellant Combustion

Grant AF-AFOSR-0897-67

March 1970

Department of Chemical Engineering

Engineering Research

College of Physical and Engineering Sciences

Brigham Young University

Final Report on

Quenching of Solid Propellant Combustion

Grant AF-AFOSR-0897-67

March 1970

Department of Chemical Engineering

This research under Grant AF-AFOSR-0897-67, Project task No. 9711-01 and for the period March 1967 through February 1970 was sponsored by the Air Force Office of Scientific Research, United States Air Force.

Technical supervisor for this program is Lt. Col. R. W. Haffner, project scientist, Propulsion Division, Directorate of Engineering Sciences, Air Force Office of Scientific Research.

Report Approved by _____

M. Duane Horton
Principal Investigator

_____

R. L. Coates
Co-Investigator

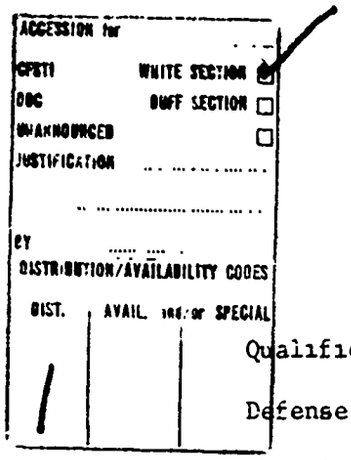

Qualified Requestors may obtain additional copies from the Defense Documentation Center. All others should apply to the clearinghouse for Federal Scientific and Technical Information.

TABLE OF CONTENTS

SUMMARY

This final report describes the progress made in the study of propellant extention under Grant AF-AFOSR-0897-67 between March 1967 and February 1969.

At the inception of the grant period, a theory had been developed to describe solid propellant flame quenching by rapid depressurization. Comparison between theory and experiment seemed promising, and it was necessary to determine the magnitude of certain combustion parameters. An experimental technique was devised and used to determine the critical combustion parameters. The use of these parameters then revealed a discrepancy between theoretical predictions and experimental results. In fact, the discrepancy was so great as to show the theoretical model to be invalid.

Accordingly, an improved theoretical model was developed and compared to experiment. The improved theory agreed well with experiment and also explained the causes behind some previously puzzling experimental results.

I. INTRODUCTION

This report describes research which is part of a continuing program intended to characterize propellant combustion during rapid depressurization. The research was initiated under Grant AF-AFOSR-897-65 and continued under Grant AF-AFOSR-897-67.

During the period of Grant AF-AFOSR-897-65, a simple propellant extinction theory was developed. This theory was based on a combustion model that assumed:

1. the heat conduction is one-dimensional
2. there are no reactions beneath the propellant surface
3. the thermal properties of the propellant are constant
4. the propellant is homogenous and semi-infinite
5. the heat transfer to the solid propellant surface was the same as the steady state heat transfer at the same pressure
6. the surface temperature was constant

With these assumptions, it was possible to numerically solve the heat transfer equations and describe the propellant extinction in terms of only two parameters. A dimensionless heat of decomposition and characteristic depressurization time.

Experimental extinction data were gathered to augment the data available in the literature and then these data were compared to the theory by the use of assumed heats of vaporization. The comparison was favorable in most cases but depended heavily on the value chosen for the heat of decomposition.

A simple method of doubtful reliability was used to experimentally determine the heats of decomposition for the propellants tested in this program.

Subsequent use of these values to make theoretical predictions proved discouraging, and it was at this point that the previous grant expired.

It was then necessary to find a better method for determining the propellant heat of decomposition. This was accomplished and is discussed in the next section of the paper. Use of the determined heat of vaporization showed that the theory was inadequate and hence improved extinguishment theory was derived. This theory, based on the Dennison and Baum combustion model (1), is described in section IV. As is shown in section V, the improved model agrees well with experimental observations.

II. RADIATION AUGMENTED BURNING RATE STUDIES

Since the exact value for the propellant heat of decomposition was so critical in comparing experiment and theory, it seemed desirable that the parameter be determined by a more reliable procedure. Accordingly, an experiment was devised to yield data from which the burning propellant surface temperature and heat of decomposition could be calculated.

The technique involved first determining the burning rate of propellant in a chamber whose wall temperature was fixed at different values in different tests. Then, the burning rate of the propellant was determined when the propellant was the shape of a long, thick-walled cylinder and the internal cylinderical surface burned. It was then reasoned that a simple strand of propellant burning in a chamber with cold walls experienced a net radiative heat loss and the burning rate would be smaller because of the heat loss. However, as the chamber wall temperature was raised, the point would be reached where there were no radiative heat losses and the combustion would be adiabatic. This would be exactly analogous to combustion inside a long hollow cylinder where the radiative losses would be negligible. The propellant surface temperature could be calculated from the chamber wall temperature that caused the propellant to burn at the same rate as did the internally burning cylinder. For the PBAN-AP propellant tested, Fig. 1 shows the surface temperature to be 560°C in excellent agreement with the experimental data of others (2,3).

It was found that the burning rate of the propellant increased linearly as the flux from the chamber wall to propellant surface increased. A computational scheme was developed that permitted us to calculate the heat of decomposition for the burning propellant. The scheme is outlined as follows:

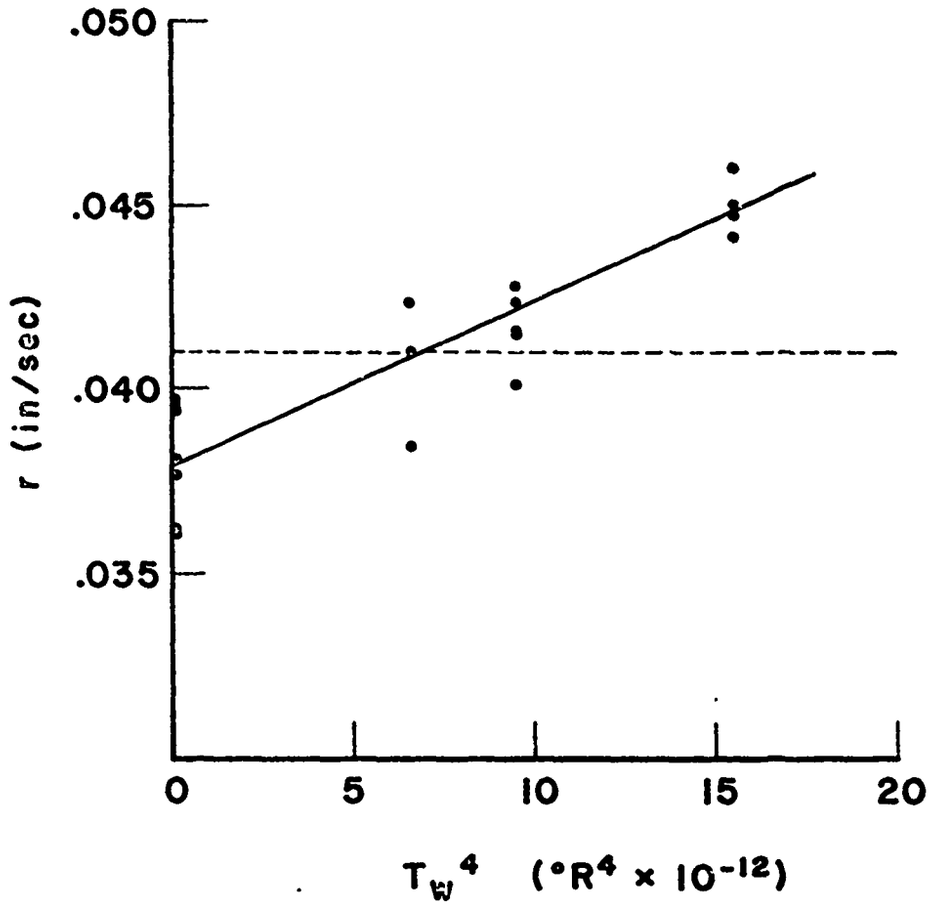

FIGURE 1 - Strand-burning rates as a function of wall surface temperature. The dotted line corresponds to the burning rate of an internal-burning cylinder.

1. The propellant burning rate ($\bar{r}$) is assumed to be a function of flame temperature (T_f) and radiant flux level (f_r) as

$$r = f(f_r, T_f)$$

2. The derivative of this equation is found to be

$$\frac{d\bar{r}}{df_r} = \frac{\partial \bar{r}}{\partial f_r} + \left(\frac{\partial \bar{r}}{\partial T_f}\right) \frac{dT_f}{df_r}$$

3. A heat balance is made at the interface; the gaseous products are assumed to have a characteristic reaction time and then the partial derivatives are written in terms of the unknown heat of decomposition (γ) and several parameters whose values are known.
4. $\frac{dT_f}{df_r}$ is evaluated from an overall heat balance.
5. The above results are combined, small order terms neglected and the resultant equation is

$$\frac{d\bar{r}}{df_r} = \frac{1}{2\rho_s [Cs(T_s - T_o) \div L]} \left[1 + \frac{C_s(T_s - T_o) + L}{C_g(T_{fo} - T_s)} \right]$$

when ρ_s is the propellant density, C_s is its heat capacity, C_g the mean heat capacity of the gases and T_s, T_o, and T_{fo} are respectively the surface temperature, the conditioning temperature, and the adiabatic flame temperature.

6. The value for the heat of decomposition, L, is found by rearranging the equation and using known values for the parameters except $d\bar{r}/df_r$, which is the slope of the heat flux-burning rate curve and is evaluated from Fig. 1.

For the propellant tested, the heat of decomposition was found to be -130 cal/g in excellent agreement with previous work (2). This number means that there is an exothermic reaction at or near the propellant surface.

The fact that the decomposition process was exothermic proved to be very significant. Previously, the decomposition was assumed to be endothermic and all calculations were made on that basis. When the correct exothermic value was used in the theory and the theoretical predictions examined, they were found to be totally unrealistic. In fact, it was found that a decrease in pressure was predicted to cause an increase in burning rate. A relation totally at variance with the known facts.

III. EXTINCTION AND OTHER COMBUSTION CHARACTERISTICS:

A readily extinguishable propellant is one whose burning rate is easily made to approach zero by a given pressure transient. Mathematically, the value of $\frac{dr/r}{dp}$ is large for such a propellant. Similarly, a propellant very susceptible to oscillatory combustion has a large value for the real part of the response function $\frac{dr/r}{dp/p}$. The similarity of the two groups suggests that a very extinguishable propellant may also be one very prone to oscillatory combustion.

This potential relationship was investigated by determining the extinction characteristics of several propellants whose oscillatory combustion was studied elsewhere (4,5). Specifically, a mesa-type base (X-14) a conventional double base (JPN) a polyurethane (JPL 534), and a polysulphide (T-35), were tested. Each of these propellants has been used in a developmental motor and each has exhibited severe oscillatory combination.

The experimental results are shown in Table 1 and clearly indicate that there is no simple relation between extinguishability and instability. In fact, the two double-base propellants are about equally unstable but differ in ease of extinguishability by two orders of magnitude.

TABLE 1

Propellant	$\left(\frac{dr/r}{dp/p}\right)_{Re}$	Critical $\frac{d\ell np}{dt}$
JPN	2.6	- 7
X-14	2.4	- 700
JPL 534	1.2	- 20
T-35	1.4	- 80

It was pointed out previously (9) that there is a correlation between extinguishability and the burning rate near the deflagration limit. However, the burning rate near the deflagration limit is a parameter rarely measured and reported. Therefore, during this period little additional data have been found. Such data as were found supported the correlation but it is concluded that at this time the use of such a seldom-measured parameter has limited utility.

IV. THEORY

1. Review of Previous Models

Mathematical models of the process of rapid depressurization extinguishment of a burning solid propellant have been proposed by at least a dozen different authors. According to a recent paper by Merkle, et. al. (6), the universal approach has been to assume that the extinguishment process occurs because of a deficiency in the heat flow from the flame to the burning surface and into the unburned solid, this heat flow being a function of the pressure. This statement applies to the present approach.

To describe the heat flow, the solid propellant is considered to be represented as a semi-infinite slab in order that only one-dimensional heat transfer need be considered. Figure (2) shows the geometrical model of the process along with the general shape of the temperature profile, which extends from the completely reacted products of combustion at the adiabatic flame temperature, T_f, to the initial conditioning temperature of the propellant, T_o. For further simplification, the burning surface is taken as the reference point for the position coordinate x, the propellant assumed to move to the left at its burning rate in order to maintain the burning surface at a fixed position.

An energy balance taken on an element of the solid of thickness dx results in the following partial differential equation:

$$\frac{\partial T}{\partial t} = \alpha \frac{\partial^2 T}{\partial x^2} + r \frac{\partial T}{\partial x} \qquad (1)$$

where α is the effective thermal diffusivity of the solid and r is the burning rate. This equation is easily integrated for the steady-state ($\partial T/\partial t = 0$) to yield the following equation for the temperature profile in the solid:

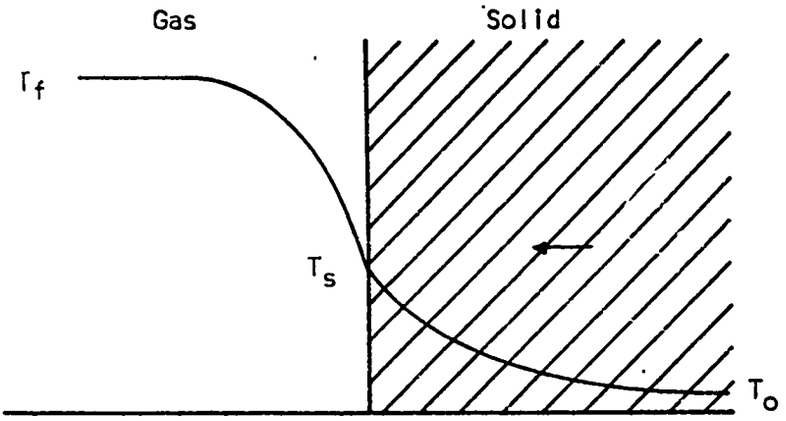

Geometrical Model of Burning Propellant

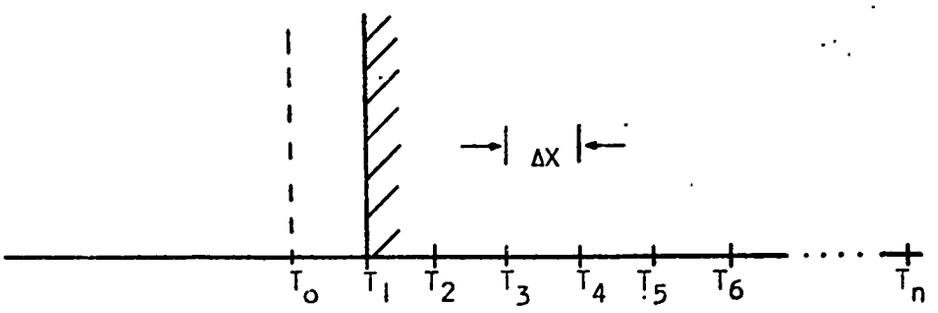

FIGURE 2 - Method of Separating Solid into Finite Difference Elements

$$T = T_o + (T_s - T_o) \exp(-\bar{r} x / \alpha) \quad (2)$$

where T_s is the temperature of the burning surface and $\bar{r}$ is the steady-state burning rate. The heat flux that must be supplied to the solid to maintain this profile, in addition to that necessary to gasify or decompose the solid, is given by

$$f_s = \rho c_s \bar{r} (T_s - T_o) \quad (3)$$

and the thermal energy stored in the solid above its initial conditioning state is

$$q_s = (k / \bar{r}) (T_s - T_o) \quad (4)$$

where k is the thermal conductivity.

The original models of Von Elbe (7) and Paul (8) were the first to consider the non-steady-state heat flow problem with the objective of predicting extinguishment conditions. These models are very similar and do provide insight into the physical processes that might lead to extinguishment even though they are based on rather gross simplifying assumptions. The Paul model is outlined here to provide a historical reference for comparison with the model developed for this study.

Paul assumed that as a first approximation the surface temperature remained constant. He further took the steady-state burning rate to be related to the pressure by

$$\bar{r} = a p^n \quad (5)$$

and assumed that the flux into the solid during either steady-state or transient periods could be expressed as

$$f_s = \rho\, c_s \bar{r} (T_s - T_o) \tag{6}$$

For a transient case, $\bar{r}$ would be interpreted as the steady-state rate corresponding to the instantaneous value of the pressure. During a transient period, the energy stored in the solid must change as the burning rate changes. Both Von Elbe and Paul assumed as a first approximation that this stored energy adjusts instantaneously with changes in burning rate, its magnitude always being given by Equation 4. Thus, during a transient period, the required flux is

$$f_s = \rho\, c_s r (T_s - T_o) + dq_s/dt \tag{7}$$

Combining (4) and (5) and carrying out the differentiation yields

$$dq_s/dt = - \frac{nk}{\bar{r}} (T_s - T_o) \frac{d\ln p}{dt} \tag{8}$$

and combining (6), (7), and (8) yields

$$r = \bar{r} \left[1 + (n\alpha/\bar{r}^2) \frac{d\ln p}{dt}\right] \tag{9}$$

Equation 9 predicts that the instantaneous rate will drop to zero whenever

$$\left(\frac{d\ln p}{dt}\right)_{Ext.} = - \bar{r}/n\alpha \tag{10}$$

Since it was observed that this equation only qualitatively correlated experimental extinguishment data, a correction factor, λ, was added to bring it into quantitative agreement, or

$$\left(\frac{d\ln p}{dt}\right)_{Ext.} = - \lambda\bar{r}/n\alpha \tag{11}$$

Horton (9) recognized that a serious shortcoming of the Paul and Von Elbe theories was the assumption that the heat stored in the solid adjusted instantaneously to changes in burning rate. In reality when a change in pressure and corresponding heat flux to the solid occurs there is a time lag before a new steady-state profile is established. To treat the transient conduction process more exactly, Horton carried out a numerical integration of the non-steady-state differential energy balance equation (Equation 1). He further improved the theory by including the energy required for gasification of the solid in the solid heat flux equation. His equation, corresponding to Equation 6, for the flux supplied to the solid is

$$f_s = \bar{r}\,\rho\,[L + C_s(T_s - T_o)] - r\,\rho L \qquad (12)$$

where L is the effective heat of gasification of the solid. The flux required by the solid in Horton's model, corresponding to Equation 7, is obtained from the numerical integration of the differential energy balance. As in the Paul model, the criterion for extinguishment is that the rate becomes zero as a consequence of the supplied f_s being entirely absorbed by the solid in changing q_s, the amount of heat stored.

Horton's model predicts for an exponential pressure decay and for a given T_f and T_s that

$$\left(\frac{d \ln p}{dt}\right)_{Ext.} = - \lambda_H(\bar{r}^2/\alpha) \qquad (13)$$

where λ_H is a function of n, L_s, and P_a/P_o, the latter being the ratio of the final pressure following depressurization to the initial pressure. The function λ_H is described in terms of graphs developed from the results of the numerical calculations.

Comparing (13) with (11) shows that λ_H corresponds to the correction factor λ employed with the Paul theory. Thus, Horton's theory provides a method of evaluating λ in terms of more fundamental parameters.

During the course of the present contract, it was discovered that Horton's model yielded erroneous results if the heat of gasification, L, were negative. This was considered to be a serious shortcoming since, as discussed in Section II, there is evidence suggesting this parameter can indeed be negative for some propellants.

More recent models have been proposed by Wooldridge (10) and by Summerfield (11). The latter model is based upon the Granular Diffusion Flame Theory of Summerfield, which does not provide the proper dependence of steady-state burning rate on pressure for many propellants. Wooldridge's approach was to modify a combustion theory originally proposed by Denison and Baum (1). This same approach has been followed in the present study. The unique feature of the present approach is that the Denison-Baum theory is used only to predict deviations from the steady-state conditions; the conventional steady-state strand-burner data is employed as fundamental input data.

2. Development of Present Model

The Denison-Baum model was originally derived as a simplified transient combustion model for application to combustion instability problems. Rather than employing a constant burning surface temperature, as Horton did, this model uses an Arrhenius-type relationship between burning rate and temperature.

$$r = A \exp\left(-E_s/RT_s\right) \tag{14}$$

It is further assumed that the rate is coupled to the flame temperature, T_f, and pressure by the following equation

$$r = BP^N T_f^{N+1} \exp (E_f/RT_f) \tag{15}$$

In the present analysis these equations have been replaced with

$$r = \bar{r}_p \exp [(-E_s/R) (1/T_s - 1/\bar{T}_{s,p})] \tag{16}$$

and

$$r = \bar{r}_p (T_f/\bar{T}_f)^{n+1} \exp [(-E_f/R)(1/T_f - 1/\bar{T}_{f,p})] \tag{17}$$

where $\bar{r}_p$, $\bar{T}_{s,p}$, and $\bar{T}_{f,p}$ are the steady-state burning-rate, surface temperature, and flame temperature at the instantaneous pressure p, and n is the empirical value of $d\ln\bar{r}_p/d\ln p$.

The most important feature of the Denison-Baum theory is the equation for the rate of heat conduction into the solid beneath the burning surface. This equation may be written as

$$k \left.\frac{\partial T}{\partial x}\right| x = 0 + = -r\rho_s [C_s (T_s - T_\infty) + C_g (\bar{T}_f - T_f)] \tag{18}$$

with the origin of the x coordinate fixed on the burning surface, the positive direction extending into the solid. This equation is obtained by combining overall energy balances for both steady and non-steady conditions, eliminating energy terms associated with the surface gasification reaction. The virtue of this equation is that data for surface and flame temperatures are more readily available than data for effective heats of gasification. Calculation of the numerical value of the instantaneous heat-flux supplied to the solid is also straight-forward. Given instantaneous values of T_s and P, r is computed from (16) and T_f is computed from (17). These values then given the instantaneous value of the flux to the solid when substituted into (18).

The most difficult problem in employing either the Horton or the Denison-Baum models in predicting extinguishment conditions is the calculation of the rate of transient heat conduction into the solid propellant. The usual numerical technique for solving the differential energy balance which describes the transient heat transfer process, Equation (1), is to separate the solid into finite difference elements such that the energy balance on each element can be written as an algebraic equation rather than a differential equation. The algebraic equations, one for each of the finite elements, are then solved simultaneously to obtain both the temperature profile at any given instant during the transient period and the increment of change at any position for a given increment in time.

Since sophisticated numerical techniques have become available for the simultaneous solution of a set of ordinary differential equations, two recent authors (12, 13) have pointed out the advantage of using these techniques to solve transient heat conduction problems. The differential energy balance for both finite elements is transformed into an ordinary differential equation applying finite difference methods to the space derivatives only. Available differential equation-solving programs are then employed to carry out simultaneous integration of these equations to compute the variation of the temperature profile with time. This approach has been adopted in this study.

Figure 2 illustrates the method of separating the solid into finite elements. The ordinary differential equation which approximates the energy balance for each element is written as

$$\frac{dTi}{dt} = \alpha\left[\frac{T_{i-1} - 2T_i + T_{i+1}}{(\Delta X)^2}\right] + r\left[\frac{T_{i+1} - T_{i-1}}{2\Delta X}\right] \qquad (19)$$

The wide variation of r during the extinguishment transient presents special problems in the numerical solution of the transient conduction equation. This problem is illustrated by considering the change in the depth of penetration of the temperature profile during the transition from one steady-state condition to another, the first condition being that prior to depressurization and the other the condition after a depressurization has occurred, the propellant assumed to continue burning. The steady-state temperature-profile is described by

$$\frac{\bar{T} - T_\infty}{T_s - T_\infty} = \exp\ (-\bar{r}x/\alpha) \tag{20}$$

Suppose that during the transient the rate is reduced by a factor of 10. Equation (21) shows that the depth at which a given temperature is established in the solid is then increased by a factor of 10. Suppose further that 20 equal elements of width ΔX are selected at the start, the final element chosen such that its temperature rise was only 5% of the rise at the surface. The temperature rise of this element when the new steady-state is established would be 74% of the surface rise; 200 elements of width ΔX would now be required to reach a depth where the rise was only 5%. Since a separate equation must be solved for each element, the problem can become unwieldy if equal-sized elements are employed and the burning rate change is large.

Marxman and Wooldridge (10) suggests that the problem of excessive finite elements can be circumvented by employing the transformation

$$1 - Y = \exp\ (-rx/\alpha) \tag{21}$$

to define a new distance variable Y. This variable ranges from 0 to 1 as X ranges from 0 to ∞, and elements of equal width ΔY correspond to ΔX elements

which become successively wider as X increases, the last element having the width α. This transformation has been investigated during this study and found to lead to erroneous results if the rate varies widely. A different transformation has been found to better accomplish the desired reduction in finite elements and also retain the accuracy of the numerical integration method. In this transformation the new distance variable, y, is defined by

$$\frac{dy}{dx} = \frac{r}{\alpha} (1 - y) \tag{22}$$

The corresponding finite element spacing is

$$\Delta x = (\alpha/r)\ \Delta y/(1 - y) \tag{23}$$

Letting y range between zero and one and taking Δy as a fixed quantity, the finite difference spacing, Δx, increases regularly with both increasing depth beneath the surface and decreasing burning rates. The resulting finite difference equation in non-dimensional form that was used in place of Equation (1) is

$$\frac{d\theta_i}{d\tau_s} = a_i R^2(\theta_{i-i} - \theta_i + \theta_{i+1}) - b_i c_i(\theta_{i+1} - \theta_{i-1})\ (1/R)\ \frac{dR}{dT_s} \tag{24}$$

with

$$\theta_i = T_i/T_o$$

$$\tau_s = \bar{r}^2 t/\alpha$$

$$R + r/\bar{r}$$

$$a_i = (1 - y)(1 - y_i - \Delta y/(\Delta y)^2 \tag{25}$$

$$b_i = \sum_{j=o}^{i} \Delta y/(1 - y_i)$$

$$c_i = (1 - y_i)(1 - y_i - \Delta y)/(2 - 2y_i + \Delta y)$$

The last term on the right-hand side of Equation (25) accounts for adjustment of the temperature as the mid-point of the finite element is shifted along the x axis due to changes in r. This term does not appear in the equation for the surface temperature (which becomes T_1) since this point is stationary.

The surface boundary condition, Equation (18), was expressed in finite-difference form by defining a station at a position y above the surface with a fictitious temperature T_o:

$$T_o \equiv T_2 + 2\Delta x_o \left(k\frac{\partial T}{\partial x}\right)_{x=o+} \tag{26}$$

where T_2 is the temperature at the first station beneath the surface.

Initial calculations were made solving Equations 16, 17, 18, 24, 25, and 26 simultaneously along with the following equation describing an imposed depressurization rate.

$$\frac{dP}{d\tau_s} = - (P - P_A)(0.693/\tau_{\frac{1}{2}}) \tag{27}$$

A standard computer program for integrating simultaneous ordinary differential equations based on Adams method (15) was employed The Fortran Coding for carrying out these calculations using the BYU Librascope L-3055 computer is included in the Appendix.

V. COMPARISON BETWEEN THEORY AND EXPERIMENT

A series of parametric calculations have been made both to determine a consistent set of parameters for correlating observed extinguishment conditions and to determine the sensitivity of the model to variations in the individual parameters.

A rough correlation of existing depressurization extinguishment data is shown in Figure 3, where the time corresponding to reducing the pressure to one-half the initial value is plotted versus the initial burning rate. The data points represent limiting conditions for extinguishment to occur. If $t_{1/2}$ is greater than that indicated by the data point and the initial rate is the same, the propellant will continue to burn rather than extinguish.

The line correlating this data can be represented by the equation

$$t_{1/2} = 0.5/\bar{r}^2 \tag{28}$$

where $t_{1/2}$ is in milliseconds and $\bar{r}$ is in inches per second. The rate of depressurization is assumed exponential with P_a/P_o assumed negligible compared to unity.

The non-dimensional half-time corresponding to (28) is

$$\tau_{1/2} = 0.5(10^{-3})/\alpha \tag{29}$$

Thus, if α is again assumed to be $2.5(10^{-4})$ in.^{2}/sec., the value of $\tau_{1/2}$ corresponding to extinguishment is 2.

Figure 4 shows predicted burning rates during depressurization transients for $\tau_{1/2} = 1.5$ using the following set of parameters:

$$Es = 30 \text{ Kcal/gm. mole}$$

$$Eg = 30 \text{ Kcal/gm. mole}$$

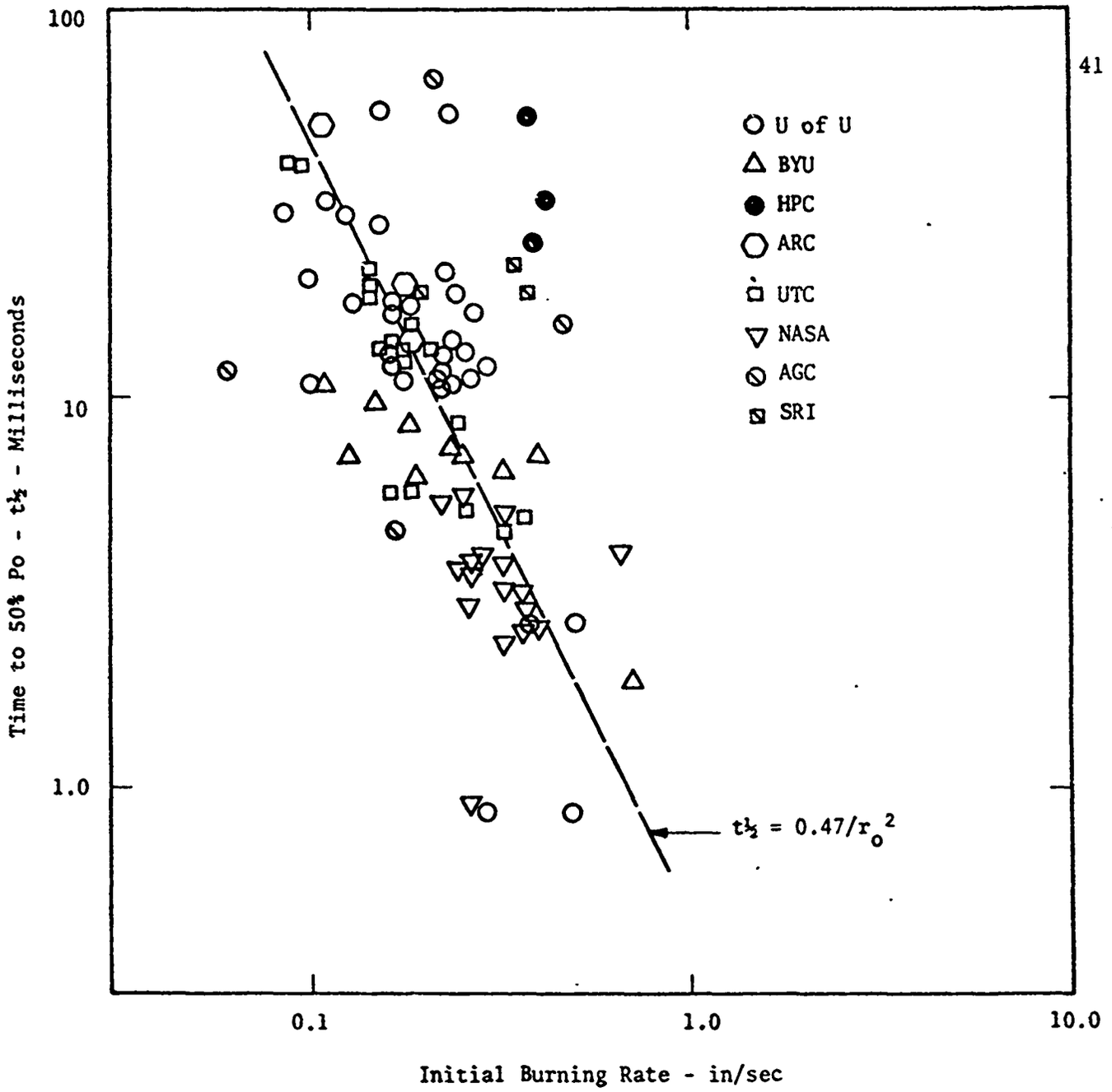

FIGURE 3 - Results of attempt to correlate marginal $\dot{p}$ extinguishment with initial burning rate

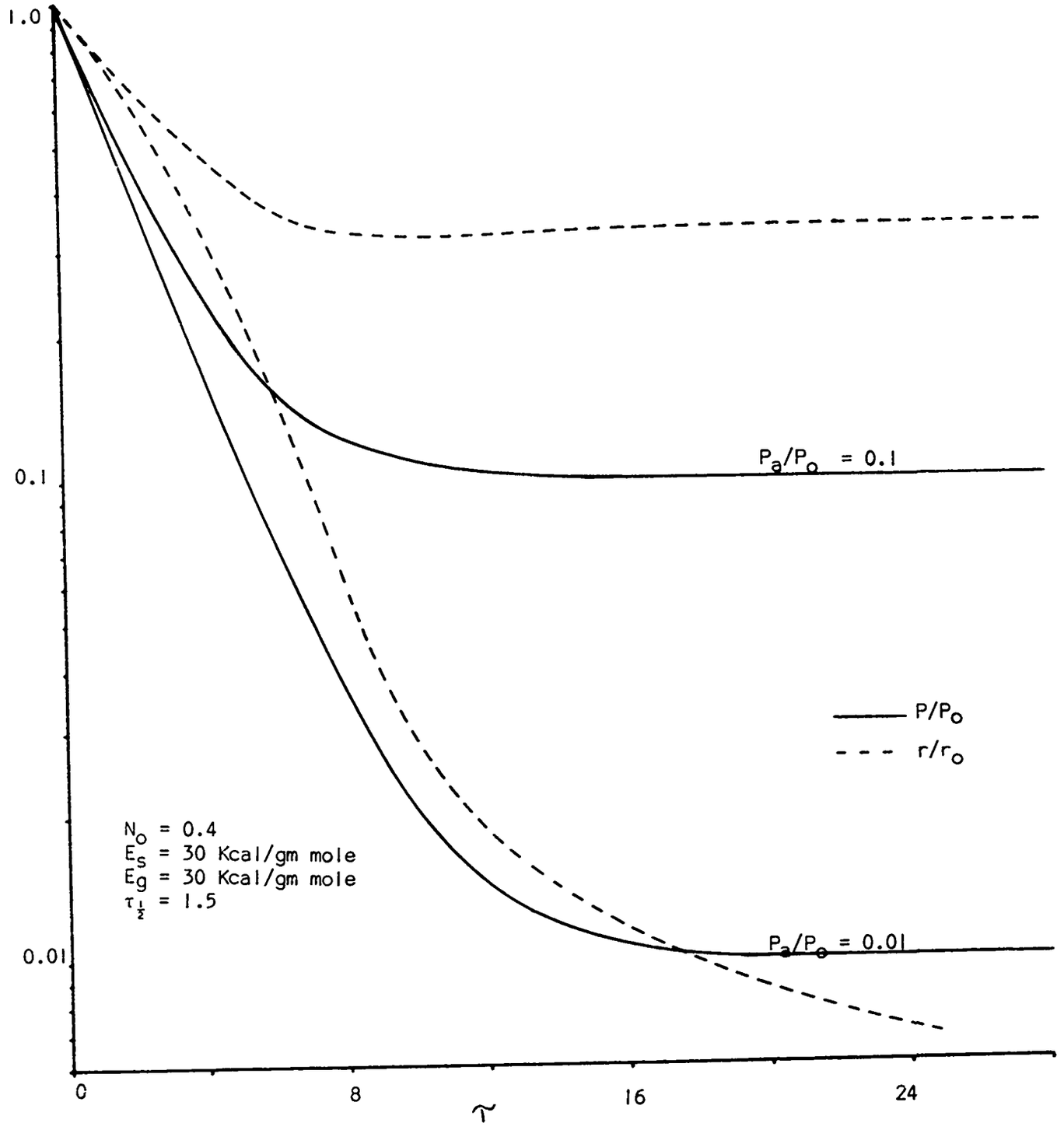

FIGURE 4 - Predicted Termination Transients for $\tau_{\frac{1}{2}} = 1.5$.

$$T_o = 298°K$$

$$T_f = 10\ T_o$$

$$T_s = 3\ T_o$$

$$n = 0.4$$

$$P_a/P_o = 0.1,\ 0.01$$

$$C_g/c = 1.0$$

The burning rate is shown to establish a new steady-state value following depressurization to $P_a/P_o = 0.1$; however, it is shown to continue to decrease following depressurization to $P_a/P_o = 0.01$, the ratio r/F dropping far below the value corresponding to steady-state at the pressure following depressurization. This latter behavior is considered to represent the extinguishment process, the reasoning being that combustion will not be sustained below some absolute minimum rate (or absolute minimum Ts). For example, if the initial rate were 0.2 inches per second, the predicted rate for the case of P_a/P_o = 0.01 at $\tau = 24$ is 0.0014 inches per second. Since rates this low are not observed experimentally during steady-state conditions, it seems improbable that rates this low would exist during a transient condition. Thus it is predicted that if $\tau_{\frac{1}{2}} = 1.5$ extinguishment would become marginal at some value of P_a/P_o lying between 0.01 and 0.1 for this particular set of propellant parameters, and since $\tau_{\frac{1}{2}} = 2.0$ is required to correlate the experimental data, as discussed above, this particular combination of parameters yields reasonably good agreement between theory and experiment.

A series of computations has been made to determine the effect of varying the gas-phase and solid-phase global activation energies. The results of these

calculations are shown in Figures 5 and 6. Increasing either E_s or E_g is shown to result in greater susceptibility to extinguishment. This effect is most strikingly shown in Figure 5 where with $E_g = 15$ a new steady-state burning rate is established following depressurization while with $E_g = 30$ the rate continues to decrease.

Figures 7, 8, 9, and 10 present the results of a series of calculations where P_a/P_o and $\tau_{\frac{1}{2}}$ were systematically varied. These calculations show a rather strong dependency of the value of $\tau_{\frac{1}{2}}$ required for extinguishment on P_a/P_o. Assuming that extinguishment corresponds to the case where $r/\bar{r}$ is predicted to drop below 0.05, the following table summarizes the predicted conditions for extinguishment derived from this set of calculations.

P_a/P_o	$(\tau_{\frac{1}{2}})$ Extinguish
0.01	10-20
0.05	1-3
0.10	0.1-0.5
0.50	< 0.01

These results suggest that the $\tau_{\frac{1}{2}}$ required for extinguishment varies roughly with the inverse square of P_a/P_o. This information may provide some explanation for the scatter in the correlation of experimental data shown by Figure 3.

The model for the solid propellant combustion process has also been combined with equations describing the transient ballistics of a solid rocket motor. Equations expressing conservation of both mass and energy inside the motor cavity have been derived previously (14). In the present study these equations have been used in the following form:

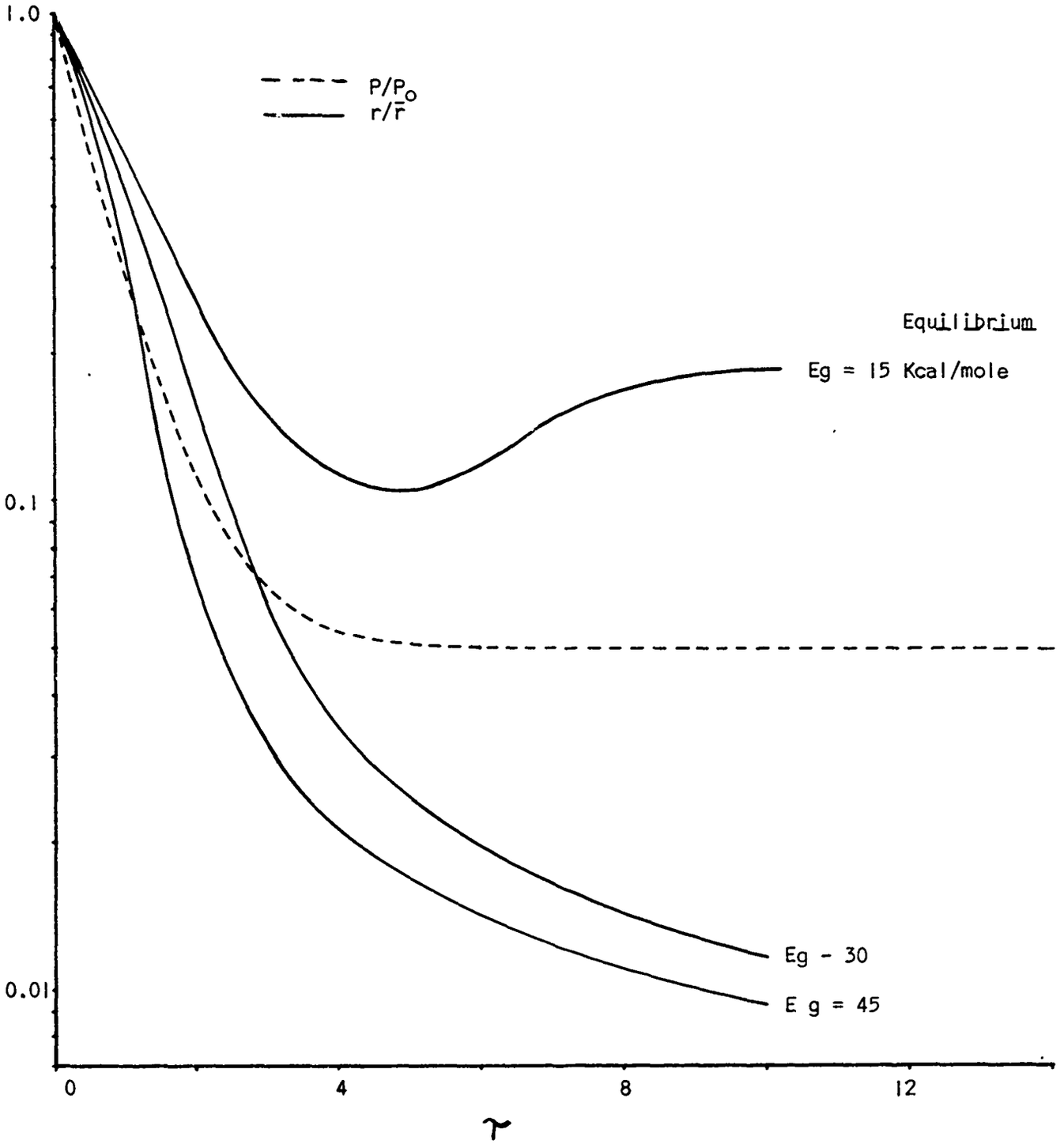

FIGURE 5 - Predicted Effect of Varying E_g

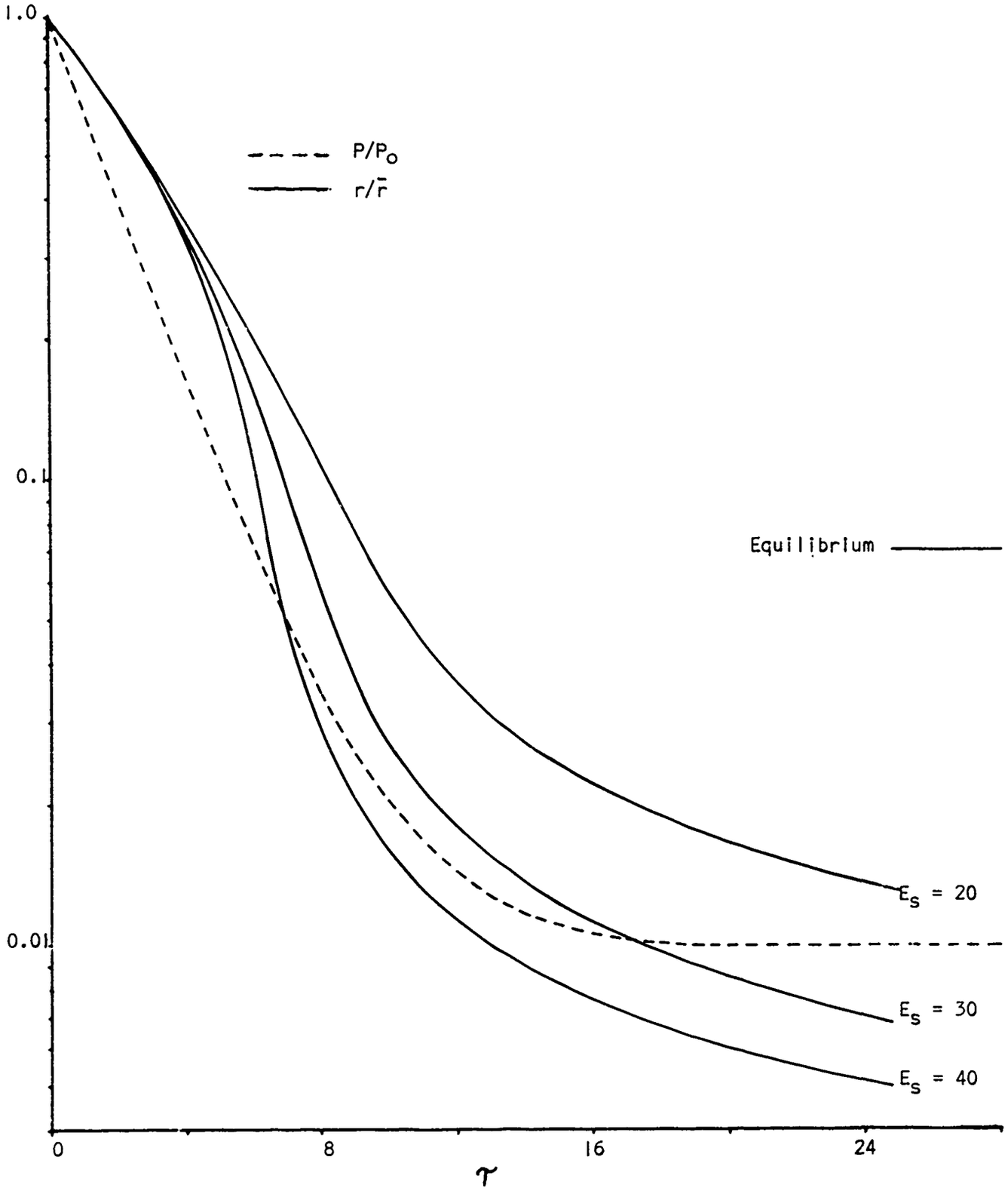

FIGURE 6 - Predicted Effect of Varying E_s

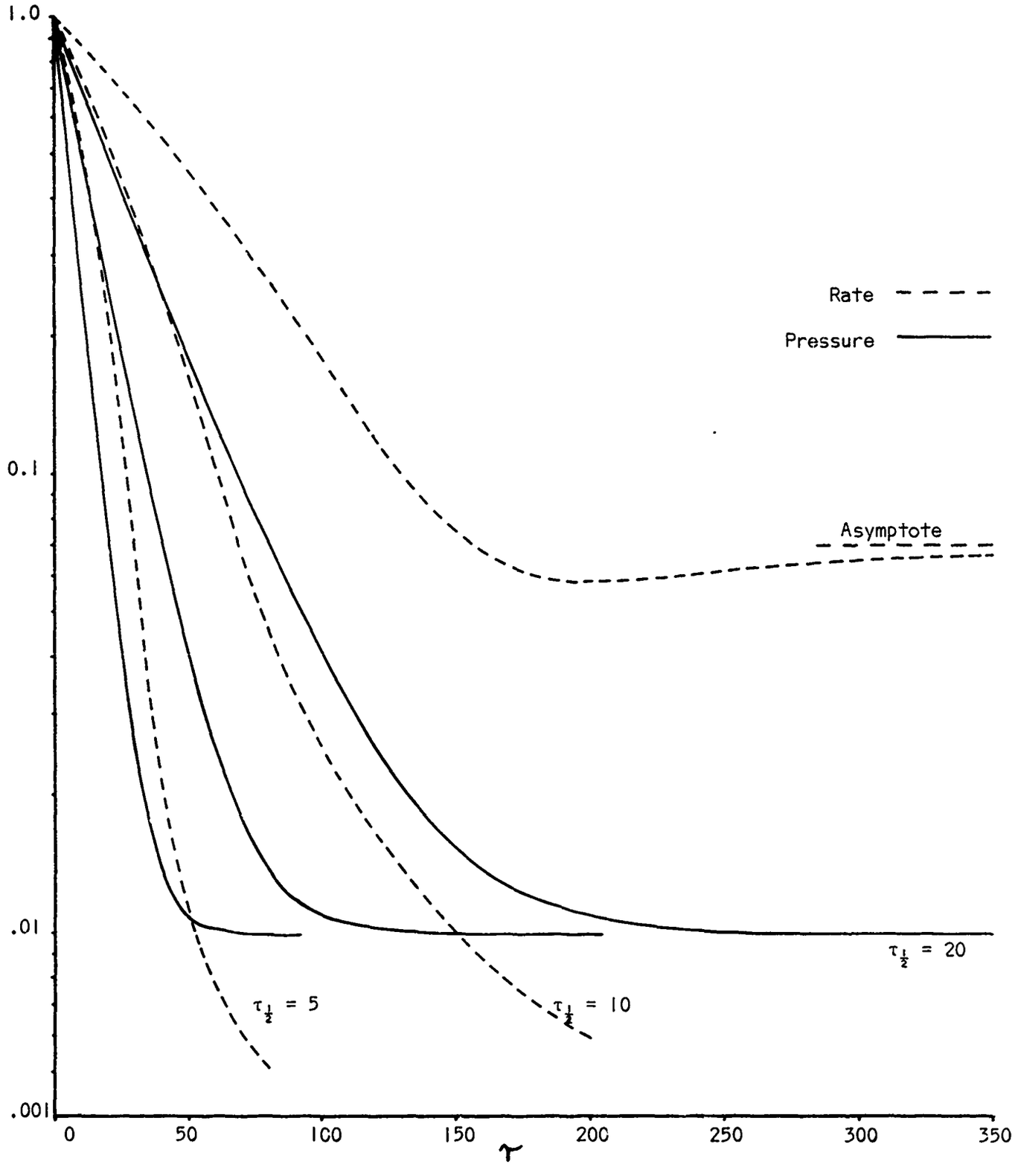

FIGURE 7 - Predicted Effect of Varying $\tau_{\frac{1}{2}}$ for $P_a/P_o = 0.01$

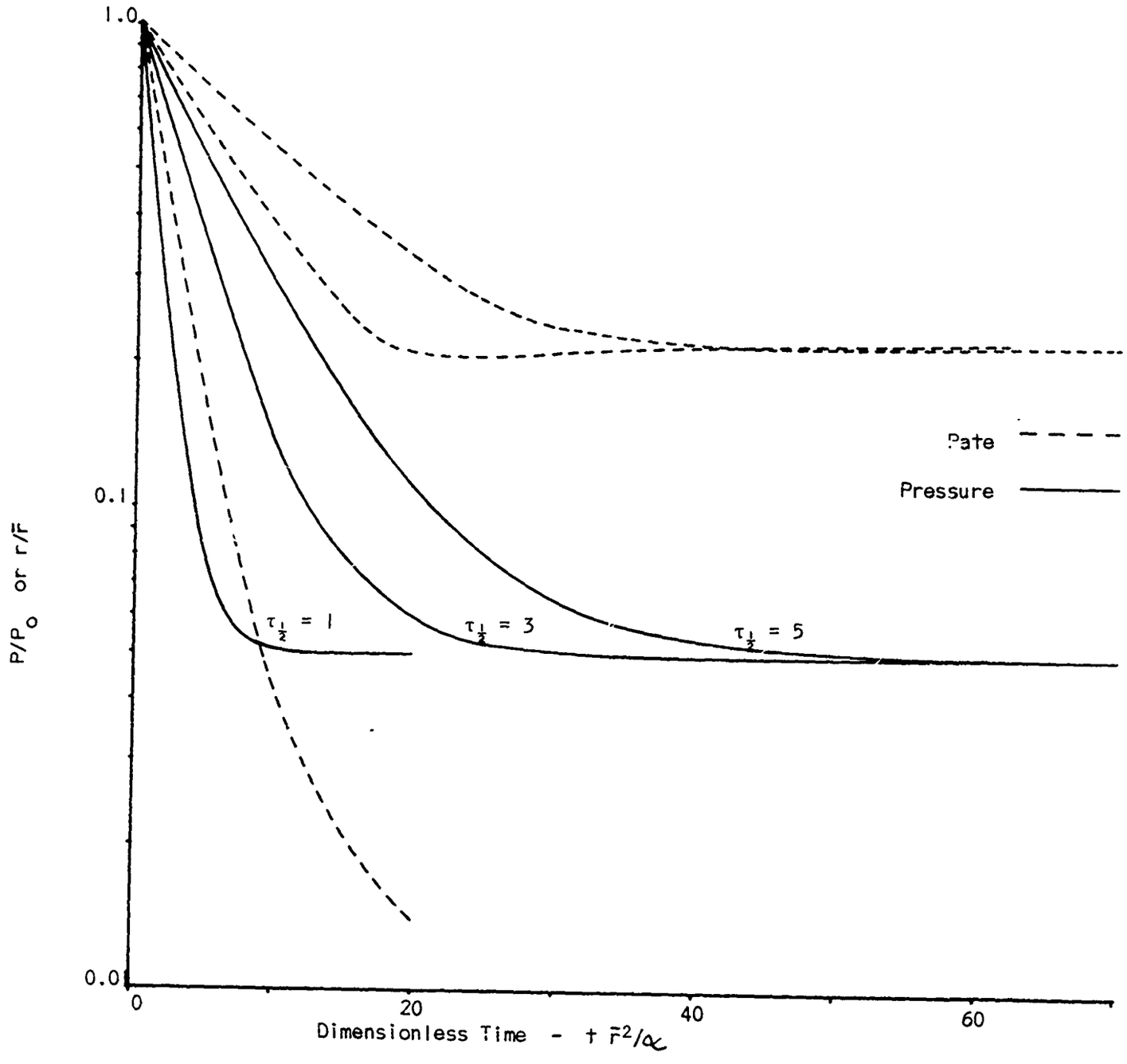

FIGURE 8 - Predicted Effect of Varying $\tau_{\frac{1}{2}}$ for P_a/P_o = 0.05

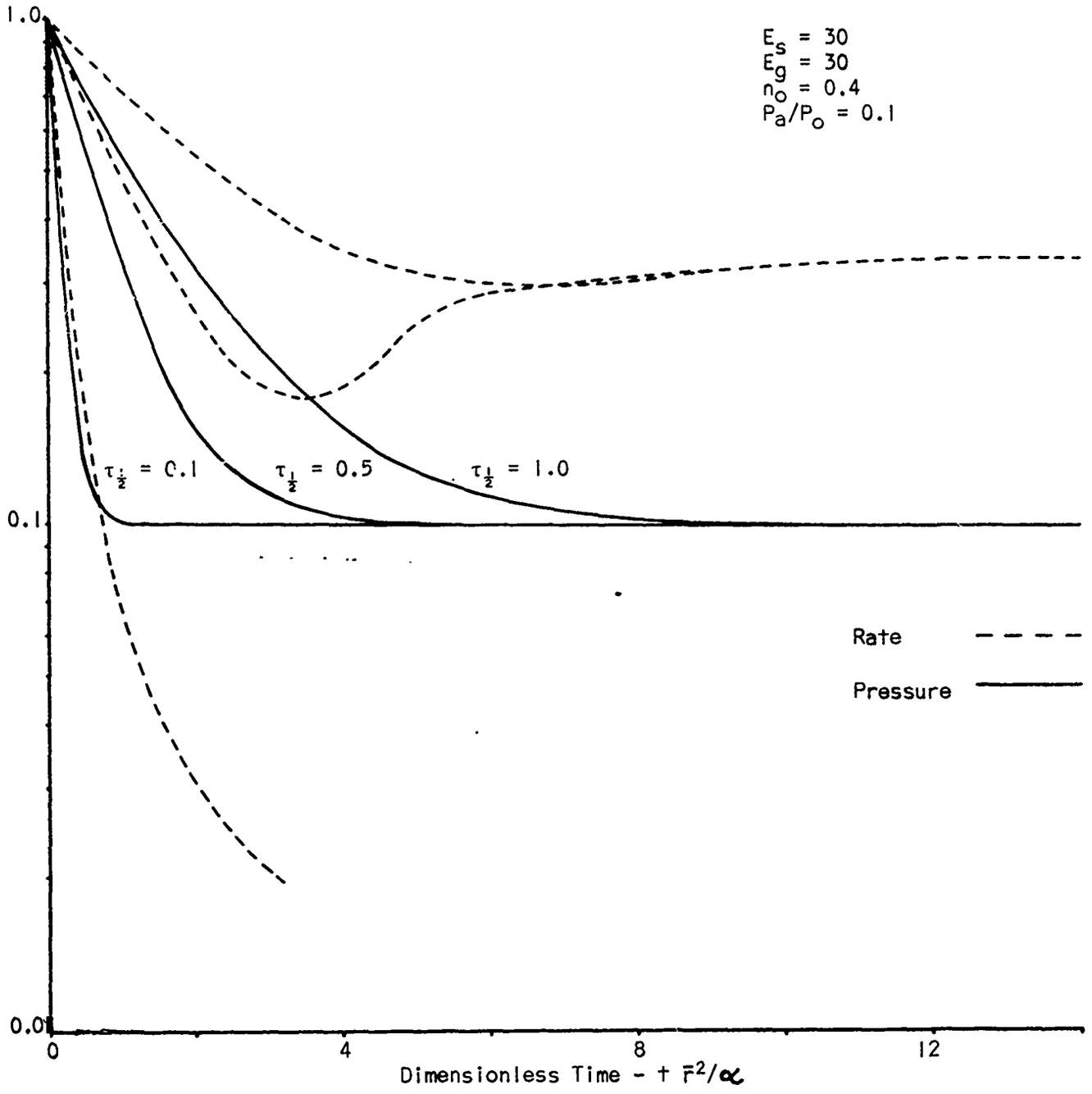

FIGURE 9 - Predicted Effect of Varying $\tau_{\frac{1}{2}}$ for P_a/P_o = 0.1

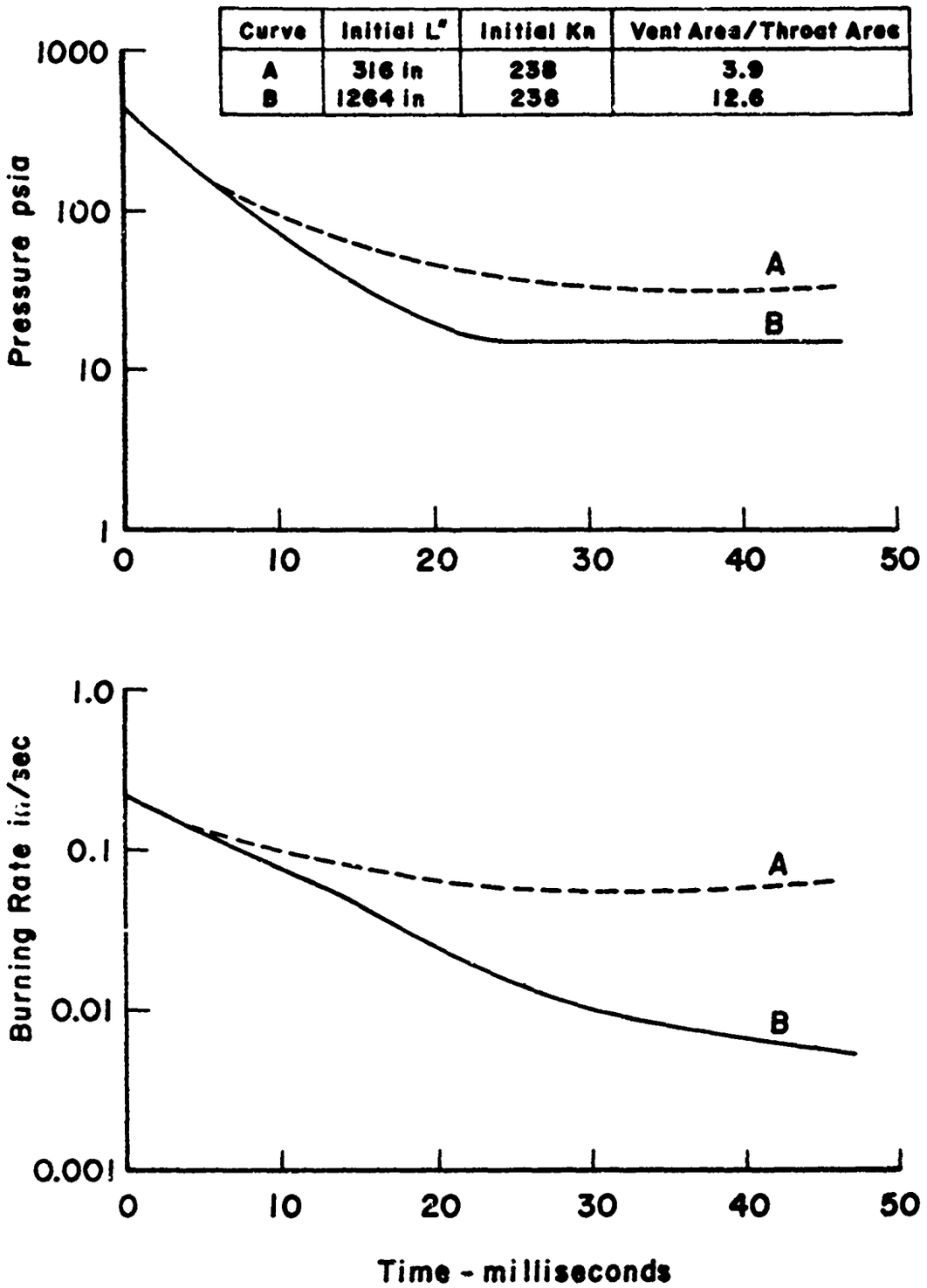

FIGURE 10 - Predicted termination transients showing the effect of varying the initial L*, the initial K_n and dP/dt constant

$$dP/d\tau_c = \gamma R\theta_f/\bar{\theta}_c)(1-(\theta_c/\theta_f)(R_N/R) \tag{30}$$

$$d\theta_c/d\tau_c = (\theta_c/P)(\theta_c/\bar{\theta}_c)(R)[1-\gamma+(\frac{\gamma\theta_f}{\theta_c}-1)(R/R_N)] \tag{31}$$

with

$$P = p/\bar{p}$$

$$\tau_c = t/(L^*/r^2C^*)$$

$$\gamma = (C_p/C_v)_{gas}$$

$$\theta_f = T_f/\bar{T}_f$$

$$\theta_c = T_c/\bar{T}_f$$

$$R_N = (\bar{\theta}_c/\theta_c)\tfrac{1}{2}PA$$

$$A = (A_{vent} + A_t)/A_t$$

Prediction of the instantaneous pressure versus time requires the simultaneous numerical integration of these equations along with those discussed earlier for the solid and the use of the steady-state burning relation. Provision has been made in the program to use the Summerfield Equation, the Vielle equation, or a table relating the burning rate to pressure. In all three cases, extinguishment is taken to occur if the rate becomes less than the burning rate at the deflagration limit of the propellant.

Tables II and III show results of calculations made with the combined combustion-ballistics model.

Table II

Predicted effect of various parameters on extinguishment of a propellant that follows the Summerfield burning rate equation

Parameter Varied	Conditions for Marginal Extinguishment: Vent-Area Rates A_2/A_1	Initial Depressurization Rate $-(p/p)_o$
Reference*	2.8-2.9	145-152
To = 100°C	3.6-3.7	204-211
$E_s = E_g = 25$	2.7-2.8	137-145
$E_s = 28$	2.7-2.8	137-145
$E_g = 28$	2.7-2.8	137-145
$E_s = 35$	2.7-2.8	137-145
$E_g = 35$	2.5-2.6	125-130
$T_s = 382$	3.7-3.8	211-218
$T_f = 2185°K$, L* = 364, C* = 3910	2.6-2.7	101-107
$T_f = 2185°K$, C* = 3910, Kn = 274	2.5-2.6	108-115
Kn = 275, L* = 364, Po = 667	3.3-3.4	159-166
Kn = 325, L* = 432, Po = 886	3.9-4.0	171-176
Kn = 188, L* = 250, Po = 340	2.2-2.3	121-131
Kn = 375, L* = 497, Po = 1124	4.5-4.6	179-184
Kn = 325, Po = 886	3.6-3.8	203-218
Kn = 375, Po = 1124	4.0-4.1	232-239
Kn = 188, Po = 340	2.4-2.5	106-114
Kn = 275, Po = 667	3.2-3.3	174-182
L* = 1000	4.0-4.1	80-83
L* = 105	2.2-2.3	254-274
$C_s/C_g = 1.0$	3.2-3.3	174-182
Kn = 274, C* = 3910	2.5-2.6	108-115

*The reference propellant and motor had the following properties:

To=25°C	T_s=600°C	ambient pressure=15 psia
Kn=238	P_s=.062 lbs/in^3	propellant area=8.3 in^2
L*=316 in	γ=1.22	nozzle open time=.001 sec
T_f=2910°K	C*=4500 ft/sec	burning rate at 1000 psi=.33 in/sec
C_s/C_g=.75	E_s=21 K cal	exponent at 1000 psi=.4
P_o=520 psia	E_g=21 K cal	burning rate at deflagration limit= .009 in/sec
r_o=.25 in/sec		

Table III

Effect of various parameters on extinguishment of a propellant that follows the Vielle burning rate equation

Parameters different than reference	Extinguishment A_2/A_1	Occurs between $-(\dot{p}/p)_o$
Reference*	3.2-3.3	177-185
n = .7	1.7-1.8	59-68
n = .3	9.0-9.25	554-569
burning rate at deflagration limit = .003	3.2-3.3	177-185
K_n = 415, L* = 582 ro = .144	2.7-2.8	78-82
K_n = 166, L* = 221 ro = .360	3.7-3.8	292-303
K_n = 1190, L* = 1580 ro = .0495	2.3-2.4	23-24
K_n = 131, L* = 174 ro = .480	4.2-4.3	425-499

*The reference propellant and motor had the following properties:

To = 25°C	T_s = 600°C	ambient pressure = 15 psia
K_n = 238	P_s = .062 lbs/in^3	propellant area = 8.3 in^2
L* = 316 in	γ = 1.22	nozzle open time = .001 sec
T_f = 2910°K	C* = 4500 ft/sec	rate at 520 psi = .25 in/sec
C_s/C_g = .75	E_s = 21 K cal	n = .5
P_o = 520 psia	E_g = 21 K cal	r at deflagration limit = .009
r_o = .25 in/sec		

One of the parameters noted to have a significant influence on marginal extinguishment conditions was the initial L* of the motor. Additional calculations in which this parameter was varied by a factor of 4 again showed the importance of the overall pressure drop. In these calculations the initial burning area/throat area ratio and initial depressurization rate were held constant by adjusting the venting area. The results of these calculations are shown in Figure 10. Because a much larger vent area/throat area ratio is necessary in the larger L* motor to achieve the same initial depressurization rate as the smaller L* motor, the final pressures differ in the two cases as do the final portion of the blow-down curves. The larger area ratio is seen to be sufficient to cause the pressure in the larger motor to drop to near ambient, the propellant burning rate dropping to a level consistent with extinguishment. The pressure in the smaller L* motor levels off at a new steady-state well above ambient with no indication that extinguishment would occur. If the model predicts a response that is truly indicative of the actual response in a motor, as suggested by the comparisons made above, this set of calculations clearly shows the difficulty that might be encountered in correlating data for extinguishment conditions described only in terms of the initial depressurization rate or $t_{\frac{1}{2}}$. Critical initial rates obtained with end-burning motors which usually have large L*'s should not be expected to be the same as critical initial rates obtained with motors containing internal burning cylinders, which normally have low L*'s.

Some data from References 10 and 12 are shown in Figure 11 and tend to confirm the predictions that have been made. That is, the initial depressurization rate required to extinguish a propellant in a given motor may be significantly different from that in a different motor--thus making design on the basis of dP/dt data very difficult.

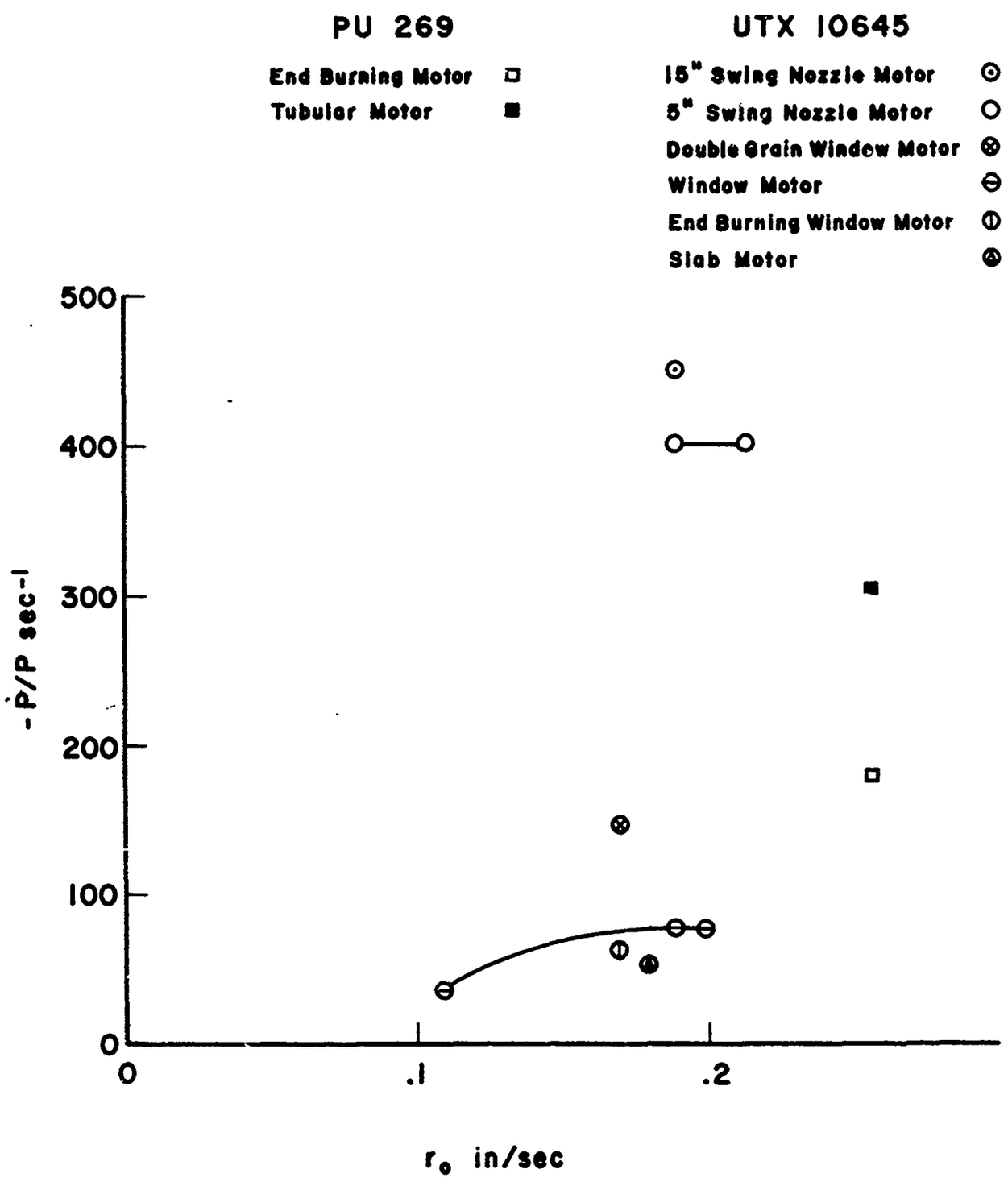

Data taken from References 10 and 12 showing that propellant in different motors requires differenct depressurization rates to be extinguished.

Figure 11

Figure 12 shows that experimental data for the effect of motor size can be correlated and also that the predictions of the improved extinguishment model are in good agreement with the experimental data. However, Figure 12 probably does not represent the best form of correlation that can be made. As is discussed in Reference 16, it appears that a simpler and better correlation relates the final L* of the motor to the final burning rate. That is, the steady-state burning rate that would result from the increased nozzle area if stable combustion resulted. Figure 13 shows results of the parametric study presented in this type of correlation.

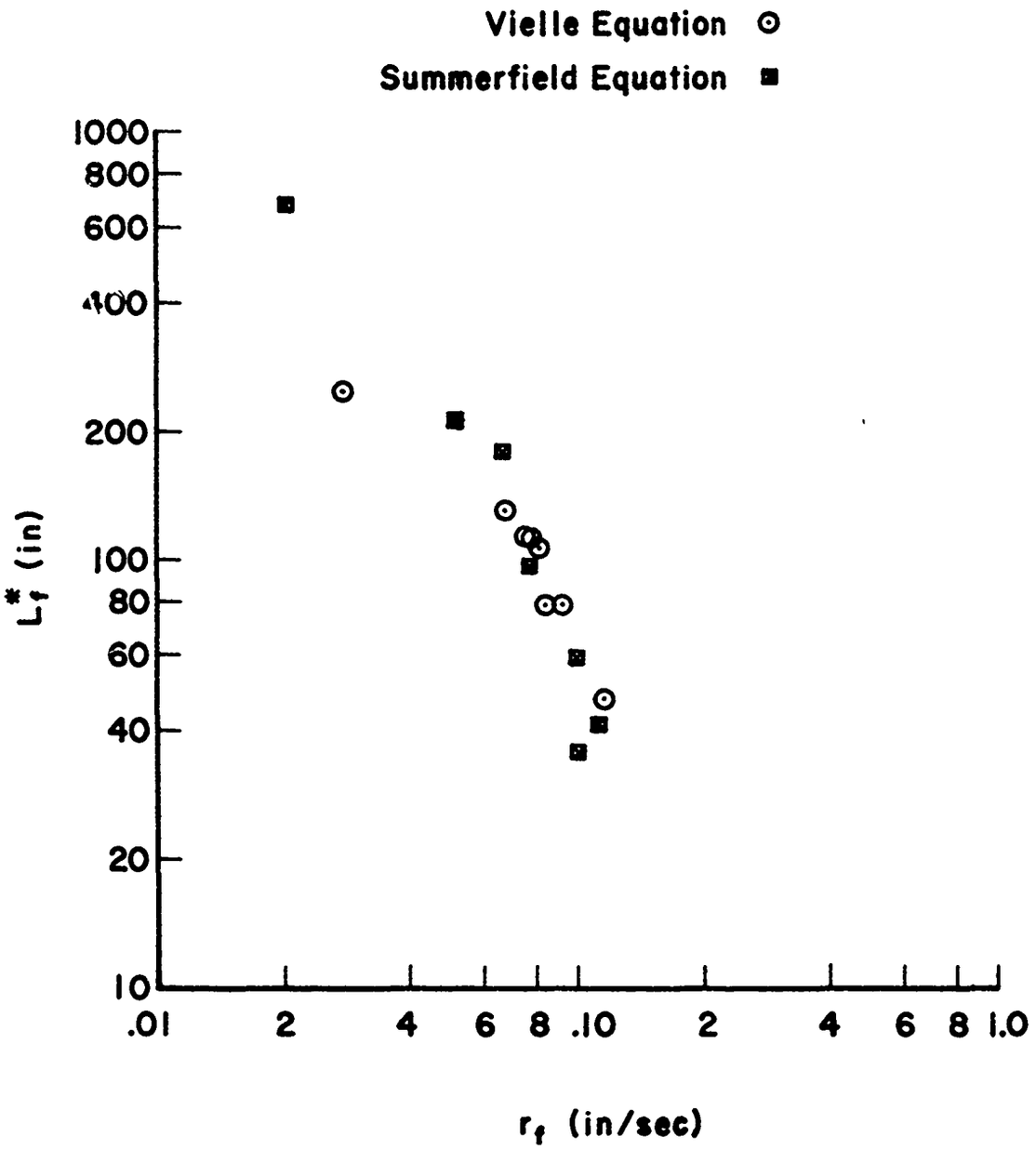

Data taken from Reference (10) and (12) showing a relation between initial pressure (P), depressurization rate (Po), burning rate ( ), thermal diffusivity ( ), chamber free volume (v), and exposed propellant surface. (Ap)

Figure 12

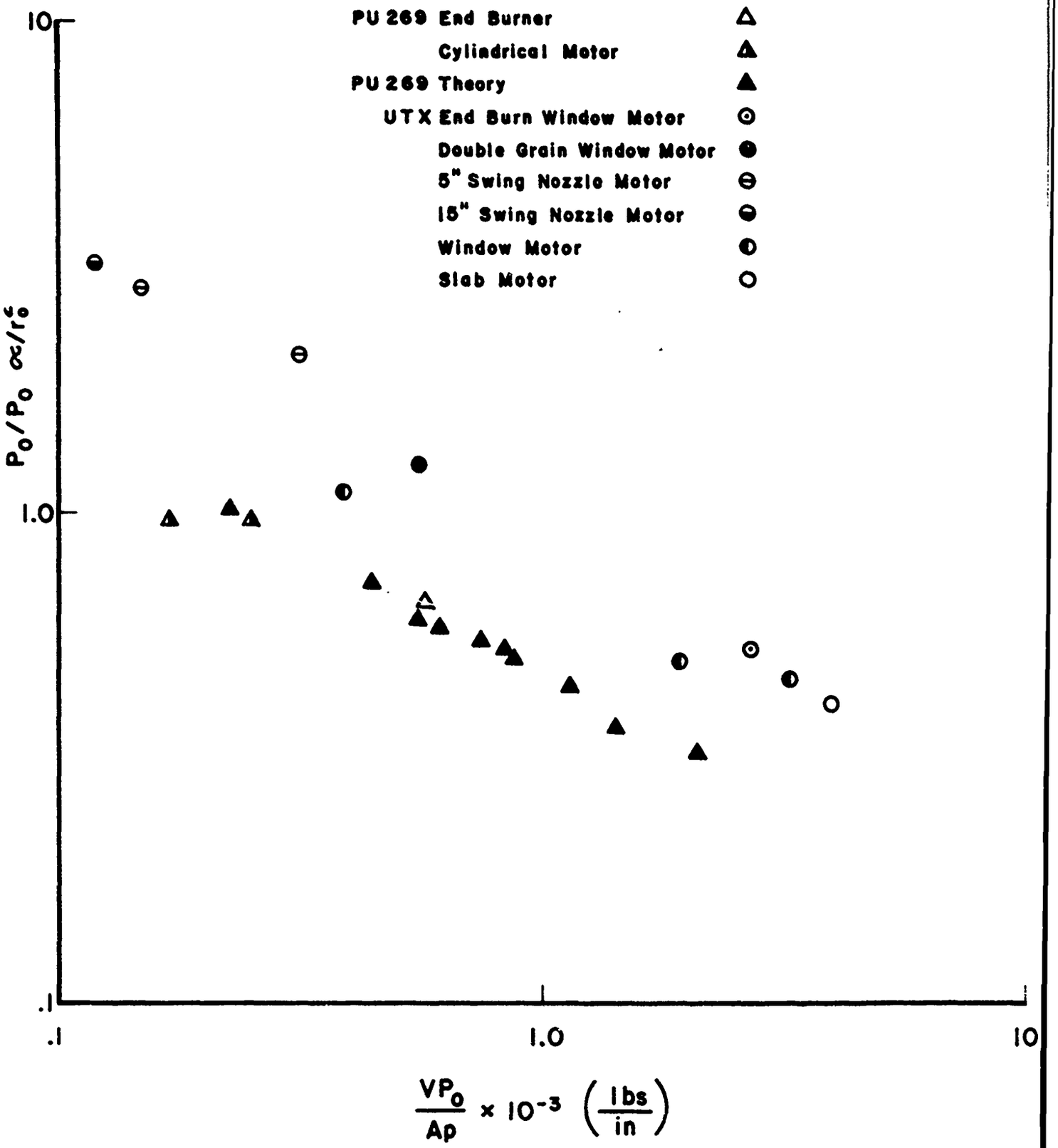

Theoretical relationship between the final conditions in a motor that marginally fails to be extinguished, for two types of steady-state burning behavior.

Figure 13

VI. CONCLUSIONS

1. It has been shown that the effect of radiation on the propellant burning rate can be used to evaluate some combustion parameters and the values can then be used to test the consistancy of a combustion model.

2. Extinguishment and oscillatory combustion were shown not to be related--at least not in a simple manner.

3. An improved extinguishment model has been developed and shown to agree well with experimental data.

VII. REFERENCES

1. Denison, M. R., and Baum, E., "A Simplified Model of Unstable Burning in Solid Propellants, J. ARS 31, 1112-1122, August 1961.

2. Sabadell, A. J., Wenograd, J., and Summerfield, M., "Measurement of Temperature Profiles through Solid Propellant Flames Using Fine Thermocouples," AIAA Journal, 3, 1580-1584 (1965).

3. Beckstead, M. W., and Hightower, J. D., "Surface Temperature of Deflagrating Ammonium Perchlorate Crystals," AIAA Journal, 5, 1875-1877 (1967).

4. Horton, M. D. and E. W. Price, "Dynamic Characteristics of Solid Propellant Combustion," Ninth Symposium (International) on Combustion, New York, Academic Press, 1963, p. 303.

5. Horton, M. D., "Testing the Dynamic Stability of Solid Propellants," NAVWEPS Report 8596, U.S. Naval Ordnance Test Station, August 1964.

6. Merkle, C. L., Turk, S. L., and Summerfield, M., "Extinguishment of Solid Propellants by Rapid Depressurization: Effects of Propellant Parameters," Preprint No. 69-176, AIAA 7th Aerospace Sciences Meeting, New York, Jan. 1969.

7. Von Elbe, G., "Theory of Solid Propellant Ignition and Response to Pressure Transients," Bulletin of the 19th ICRPG Solid Propulsion Conference (CPIA Pub. No. 18, Silver Spring, Md. 1963), Vol. III, 157-181.

8. Paul, B. E., Lovine, R. L., and Fong, L. Y., "A Ballistic Explanation of the Ignition Pressure Peak," AIAA Preprint 64-121, presented at the 5th AIAA Solid Propellant Rocket Conference (Palo Alto, Calif. Jan. 1964).

9. Horton, M. D., Bruno, P. S., and Graesser, E. C., "Depressurization Induced Extinction of Burning Solid Propellants," AIAA Journal, Volume 6, pp. 292-297, 1968.

10. Wooldridge, C. E., Marxman, G. A., and Kier, R. J., "A Theoretical and Experimental Study of Propellant Combustion Phenomena during Rapid Depressurization," Final Report Contract NASI-7349, Stanford Research Institute, Menlo Park, Calif. Feb. 1969.

11. Parker, K. H., and Summerfield, M., "Response of the Burning Rate of a Solid Propellant to a Pressure Transient," AIAA Preprint No. 66-683, presented at the Second Propulsion Joint Specialists Conference (Colorado Springs, Colorado), June, 1966.

12. "An Experimental Study of Solid Propellant Extinguishment by Rapid Depressurization," United Technology Center, Preliminary Final Report, 1969.

13. "Theoretical and Experimental Study of Extinguishable Solid Propellants," Aerojet General Corporation, Quarterly and Final Report, Contract Af 04 (611)-9889, 1965-1966.

14. Coates, R. L., Polzien, R. E., Price, C. F., "Design Procedures for Combustion Termination by Nozzle Area Variation," J. Spacecraft 3, 418-425 (1966).

15. Conte, S. D., Elementary Numerical Analysis, New York, McGraw Hill, 1965, p. 234.

16. Coates, R. L., and Horton, M. D., "Improved Design Procedures for Thrust Termination of Solid Propellant Motors," ARPL-TR-XXXX, April, 1970.

VIII. SAMPLE COMPUTER PROGRAM

```
      C     MOTOR THRUST TERMINATION
      C      R.L.COATES   REVISED OCTOBER 1969
 1          COMMON TPRNT(6),J1,J2,J3,NPTS,I,
 1         *       TO,PA,AR,XKN,ANR,TOPEN,ELSTAR,EPS,
 1         *       RBAR,RMIN,XNBAR,TFBAR,TSBAR,RHOS,GAM,CSTAR,
 1         *       ES,EG,CSCG,FEXT,ALPHA,
 1         *       CAPGAM,PCRIT,GAMF1,GAMF2,GAMF3,TCHAM,TSOL,BB,DD,TCI,
 1         *       V,P,R,DLPDT,RATE,PRESS,TF,TC,TS,TLAST,DEPTH,AN,XNP,
 1         *       TABLP(8),TABLR(8),RP
 2          COMMON J,TIME(100),PRES(100),TEMP(100),BRATE(100)
 3          DIMENSION NAME(20)
 4          READ(10)0
 5       10 J=0
 6          READ (5,13)NAME
 7       13 FORMAT (20A4)
 8          WRITE(6,16)NAME
 9       16 FORMAT (1H1,20A4)
10          N=12
11          READ(5,43) TPRNT(1),TPRNT(2),J1,J2,J3,NPTS
12       43 FORMAT (2F10.5,4I2)
13          TPRNT(3)=TPRNT(1)
14          TPRNT(5)=TPRNT(1)
15          TPRNT(4)=2.*TPRNT(2)
16          TPRNT(6)=2.*TPRNT(2)
17          IF(J2) 45,45,44
18       44 READ(5,40)TABLP
19          READ(5,40)TABLR
20       45 READ (5,40) TO,PA,AR,XKN,ANR,TOPEN,ELSTAR,EPS
21          READ(5,40) RBAR,RMIN,XNBAR,TFBAR,TSBAR,RHOS,GAM,CSTAR
22          READ (5,40) ES,EG,CSCG,FEXT,ALPHA
23       40 FORMAT (8F10.5)
24          TSOL=ALPHA/(RBAR*RBAR)
25          DO 30 I=1,6
26       30 TPRNT(I)=TPRNT(I)/TSOL
27       41 WRITE (6,42) TO,RBAR,ES,PA,RMIN,EG,AR,XNBAR,CSCG,XKN,TFBAR,FEXT,
27         *                ANR,TSBAR,ALPHA,TOPEN,RHOS,ELSTAR,GAM ,EPS,CSTAR
28       42 FORMAT(1HC,10X,'INPUT DATA'//
28         *       20X,6HTO    =,F10.3,10X,6HRBAR =,F10.3,10X,6HES    =,F10.3/
28         *       20X,6HPA    =,F10.3,10X,6HRMIN =,F10.3,10X,6HEG    =,F10.3/
28         *       20X,6HAR    =,F10.3,10X,6HNBAR =,F10.3,10X,6HCSCG =,F10.3/
28         *       20X,6HKN    =,F10.3,10X,6HTFBAR=,F10.3,10X,6HFEXT =,F10.3/
28         *       20X,6HANR   =,F10.3,10X,6HTSBAR=,F10.3,10X,6HALPHA=,F10.6/
28         *       20X,6HTOPEN=,F10.3,10X,6HRHOS =,F10.3/
28         *       20X,6HLSTAR=,F10.3,10X,6HGAMMA=,F10.3/
28         *       20X,6HEPS   =,F10.3,10X,6HCSTAR=,F10.3)
29          WRITE (6,80)
30       80 FORMAT (1H0,3X,'TIME',4X,'PRESSURE',3X,'DLPDT',7X,'RATE',5X,
30         *'SRATE',5X,'TEMPF',5X,'TEMPC',5X,'TEMPS',6X,'TLAST',4X,'DEPTH',
30         *4X,'NOZZLE',4X,'EXPONENT')
31          CALL FVFS (N,TPRNT)
32          IF(J3) 36,36,34
33       34 IF(RATE)35,35,36
34       35 ANR=0.5*ANR
35          N=12
36          GO TO 41
37       36 IF (J1) 60,60,50
38       50 WRITE (6,16)NAME
39          CALL XYPLOT (J,50,100,3,TIME,PRES,TEMP,BRATE)
```

```
  40      6?  GO TO 1?
  41          RETURN
  42          END
```

MESSAGES FOR ABOVE COMPILATION.

: VERSION 4 MOD 1

```
      SUBROUTINE SETUP (T,Y,SIG,N)
      DIMENSION T(2),Y(20),SIG(20)
      COMMON TRNT(6),J1,J2,J3,NPTS,I,
     *       TO,PA,AH,XKN,ANR,TOPEN,ELSTAR,EPS,
     *       RBAR,RHO,XNBAR,TFBAR,TSBAR,RHOS,GAM,CSTAR,
     *       FS,FG,CSCG,FFXT,ALPHA,
     *       CAPGAM,PCRIT,GAMF1,GAMF2,GAMF3,TCHAM,TSOL,RB,DD,TCI,
     *       V,P,R,DLPDT,RATE,PRESS,TF,TC,TS,TLAST,DEPTH,AN,XNP,
     *       TABLP(8),TABLR(8),RP
      COMMON J,TIME(100),PRES(100),TEMP(100),BRATE(100)
C                     REFERENCE PRESSURE IS 1000PSI
C                     REFERENCE RATE IS RATE AT 1000PSI
C                     REFERENCE CONDITIONING TEMP IS 25C
C                     CALCULATE CONSTANTS
      CAPGAM=GAM*(2./(GAM+1.))**((GAM+1.)/(GAM-1.))
      PCRIT=(2./(GAM+1.))**(GAM/(GAM-1.))
      GAMF1=SQRT(2.*GAM/(CAPGAM*(GAM-1.)))
      GAMF2=2./GAM
      GAMF3=(GAM+1.)/GAM
      AA=1.5*(1.0-XNBAR)
      BB=AA/(1.0-AA)
      DD=RHOS*XKN*CSTAR*RBAR/(1000.*32.17)
      TCHAM=ELSTAR/(CAPGAM*CSTAR*12.*DD)
      C1=FG*1000./(2.*1.98)
      I=1
      M=0
      T(1)=0.
C                     CALCULATE APPROXIMATE FLAME TEMP
      TO=TO+273.
      TFRAD=FFXT*CSCG*TO
   10 TF=TFBAR+CSCG*(TO-298.)+TFRAD
      IF(J2) 51,50,52
C                     CALCULATE INITIAL PRESSURE, SUMMERFIELD LAW
   50 XNP=XNBAR
      RT=(TF/TFBAR)**(1.+XNP)*EXP(-C1*(1./TF-1./TFBAR))
      P=(((1.+BB)*RT*DD-1.)/BB)**1.5
      CC=BB*P**0.667
      XNP=1.0-0.667*CC/(1.+CC)
      RP=P*(1.+BB)/(1.+CC)
      R=RT*RP
C                     ITERATE ON TF
   61 TFRAD=TFRAD/R
      M=M+1
      IF(M-10) 26,26,27
   26 GO TO 10
   27 GO TO 67
C                     CALCULATE INITIAL PRESSURE, VIELLE LAW
   51 XNP=XNBAR
      RT=(TF/TFBAR)**(1.+XNP)*EXP(-C1*(1./TF-1./TFBAR))
      P=RT*DD**(1./(1.-XNP))
      R=P**XNP
      GO TO 61
C                     CALCULATE INITIAL PRESSURE, P,R TABLE
   52 P=1000.
      R=RBAR/DD
   67 CALL PRATE(P,RP,XNP,TABLP,TABLR,NPTS,I)
      RT=(TF/TFBAR)**(1.+XNP)*EXP(-C1*(1./TF-1./TFBAR))
      RP=RT*RP
```

```
      IF(ABS(P-RP)-.0005)  35,35,30
   30 R=RP
      P=1.03.*RP*UD/RRAR
      GO TO 82
   35 P=P/1.03.
      R=R/RRAR
      GO TO 61
C                        CALCULATE SOLID TEMPERATURES
   40 TSBAR=TSBAR+273.
      TS=TSBAR/(1.-1.98*TSBAR*ALOG(R)/(ES*1000.))
      Y(1)=TS/TO
      T1=1.13393*Y(1)-.13393
      Y(2)=2.*Y(1)-T1
      DO 20 I=3,7
   20 Y(I)=2.*Y(I-1)-Y(I-2)
      Y(8)=(Y(7)+1.)/2.
      Y(9)=P
      Y(10)=R
      Y(11)=TF/TFBAR
      Y(12)=Y(11)
      TCI=TF
      TC=TF
      RETURN
      END
```

MESSAGES FOR ABOVE COMPILATION.

TE

026

```
C15,T=10  COATES                          FORTRAN DECK 'PRATE  '          10/24/..

   1          SUBROUTINE PRATE(P,RP,XNP,TABLP,TABLR,NPTS,I)
   2          DIMENSION TABLP(8), TABLR(8)
   3       1  IF (TABLP(I)-P) 2,4,4
   4       2  I=I-1
   5          IF (I-1) 3,3,1
   6       3  I=1
   7          GO TO 7
   8       4  IF (TABLP(I+1)-P) 8,5,5
   9       5  I=I+1
  10          IF (I-NPTS)10,6,6
  11       6  I=NPTS-1
  12          GO TO 7
  13      10  IF (TABLP(I-1)-P) 7,5,5
  14       7  XNP=ALOG(TABLR(I+1)/TABLR(I))/ALOG(TABLP(I+1)/TABLP(I))
  15       8  RP=TABLR(I)*(P/TABLP(I))**XNP
  16          RETURN
  17          END


) MESSAGES FOR ABOVE COMPILATION.

EQ                                                          026
```

```
      SUBROUTINE DIFEQ (T,Y,DYDX,N,TPR)
      DIMENSION T(2),Y(20),DYDX(20)
      COMMON TPR,T(4),J1,J2,J3,NPTS,I,
     *       TO,PA,AR,XKN,ANR,TOPEN,ELSTAR,EPS,
     *       PRAR,RMIN,XNPAR,TFRAR,TSRAR,RHOS,GAM,CSTAR,
     *       FS,EG,CSCG,FFXT,ALPHA,
     *       CAPGAM,PCRIT,GAMF1,GAMF2,GAMF3,TCHAM,TSOL,RR,DC,TCI,
     *       X,P,R,DLPDT,RATE,PRESS,TF,TC,TS,TLAST,DEPTH,AN,XNP,
     *       TABLP(8),TABLR(8),RP
      COMMON I,TIME(100),PRES(100),TEMP(100),RRATE(100)
      X=T(1)*TSOL
      P=Y(9)
      R=Y(10)
      RATE=RBAR*Y(10)
      PRESS=1000.*Y(9)
      TF=TFRAR*Y(11)
      TC=TFRAR*Y(12)
C                     CALCULATE NOZZLE AREA
      IF (X-TOPEN) 30,30,40
   30 AN=AB/XKN*(1.0+(ANR-1.0)*X/TOPEN)
      GO TO 41
   40 AN=AB/XKN*ANR
   41 A=AN/(DD*AB/XKN)
C                     CHECK FOR EXTINGUISHMENT
      IF (RATE-RMIN) 10,10,20
   10 RATE=0.
      N=0
      CALL PRINT(T,Y,DYDX,N,TPR)
      RETURN
   20 CONTINUE
C                     CALCULATE SURFACE FLUX
      FS=P*(Y(1)-1.+CSCG*(TFBAR*TO-298.-TF)/TO)*FFXT
C                     CALCULATE SURFACE TEMP CHANGE
      T1=Y(2)+0.20786*FS/R
      DYDX(1)=56.*R*R*(T1-2.0*Y(1)+Y(2))
C                     CALCULATE RATE CHANGE
      C2=1300.*FS/(1.98*TO)
      DR=R*C2*DYDX(1)/(Y(1)*Y(1))
C                     CALCULATE PRESSURE CHANGE
      RNC=SQRT(TF/TCI)*P*A
   60 PRAT=PA/PRESS
      IF(PRAT-PCRIT) 55,55,48
   48 PRATF=PRAT**GAMF2-PRAT**GAMF3
      IF (PRATF) 49,49,50
   49 RS=0.
      GO TO 51
   50 RS=RNC*EPS*GAMF1*SQRT(PRATF)
      IF (RS-RNC) 51,51,55
   51 RN=RS
      GO TO 70
   55 RN=RNC
   70 DP=TSOL/TCHAM *GAM*TC/TCI*R*(TF/TC-RN/R)
C                     CALCULATE CHAMBER TEMP CHANGE
      DTC=(TSOL/TCHAM)*TC/P*TC/TCI*R*(GAM*TF/TC-1.+(1.-GAM)*RN/R)
      IF(J2) 75,76,77
C                     CALCULATE RP,XNP  SUMMERFIELD LAW
   75 CC=RR*P**0.667
      XNP=1.0-0.667*CC/(1.+CC)
```

```
      RP=P*(1.+RR)/(1.+CC)
      GO TO 82
C                     CALCULATE RP,XNP   VIELLE LAW
   75 XNP=XNRAR
      RP=P**XNP
      GO TO 82
C                     CALCULATE RP,XNP   R,P TABLE
   77 P=1000.*P
      CALL PRATE(P,RP,XNP,TABLP,TABLR,NPTS,I)
      RP=RP/RRAR
      P=P/1000.
        GO TO 80
C                     CALCULATE FLAME TEMP CHANGE
   82 ETA=1.+XNP+1000.*EG/(3.96*TF)
      DTF=TF/ETA*(DR/R-XNP*DP/P)
C                     CALCULATE SOLID TEMP CHANGE
      DYDX(2)=42.*R*R*(Y(1)-2.*Y(2)+Y(3))-0.4615*(Y(3)-Y(1))*DR/R
      DYDX(3)=30.*R*R*(Y(2)-2.*Y(3)+Y(4))-0.8442*(Y(4)-Y(2))*DR/R
      DYDX(4)=20.*R*R*(Y(3)-2.*Y(4)+Y(5))-1.1323*(Y(5)-Y(3))*DR/R
      DYDX(5)=12.*R*R*(Y(4)-2.*Y(5)+Y(6))-1.3920*(Y(6)-Y(4))*DR/R
      DYDX(6)= 6.*R*R*(Y(5)-2.*Y(6)+Y(7))-1.3114*(Y(7)-Y(5))*DR/R
      DYDX(7)= 2.*R*R*(Y(6)-2.*Y(7)+Y(8))-1.0619*(Y(8)-Y(6))*DR/R
      DYDX(8)=.891*R*R*(Y(7)-2.*Y(8)+1.) -0.2357*(1.0-Y(7))*DR/R
      DYDX(9)=DP
      DYDX(10)=DR
      DYDX(11)=DTF/TFRAR
      DYDX(12)=DTC/TFRAR
      RETURN
      END
```

MESSAGES FOR ABOVE COMPILATION.

```
715,T=10  COATES                          FORTRAN DECK *PRINT  *          10/24/..
    1          SUBROUTINE PRINT (T,Y,DYDX,N,TPR)
    2          DIMENSION T(2),Y(23),DYDX(20),TPR(2)
    3          COMMON TPRNT(6),J1,J2,J3,NPTS,I,
    3         *       TO,PA,AB,XKN,ANR,TOMEN,ELSTAR,EPS,
    3         *       RBAR,RMIN,XNBAR,TFBAR,TSBAR,RHOS,GAM,CSTAR,
    3         *       ES,EG,CSCG,FEXT,ALPHA,
    3         *       CAPGAM,PCRIT,GAMF1,GAMF2,GAMFS,TCHAM,TSOL,BR,DC,TCI,
    3         *       X,P,R,DLPDT,RATE,PRESS,TF,TC,TS,TLAST,DEPTH,AN,XNP,
    3         *       TABLP(8),TABLR(8),RP
    4          COMMON J,TIME(100),PRES(100),TEMP(100),BRATE(100)
    5          TS=TO*Y(1)-273.
    6          TLAST=TO*Y(8)-273.
    7          DEPTH=ALPHA/RBAR*2.593/R
    8          DLPDT=DYDX(9)/(P*TSOL)
    9          SRATE=RP*RBAR
   10       14 WRITE (6,15) X,PRESS,DLPDT,RATE,SRATE,TF,TC,TS,TLAST,DEPTH,AN,XNP
   11       15 FORMAT (F10.5,F10.2,3F10.4,2F10.1,2F10.2,2F10.5,F10.4)
   12          TSTOP=TPRNT(2)*TSOL
   13          IF (X.GE.TSTOP)  N=0
   14          J=J+1
   15          TIME(J)=X
   16          PRES(J)=P
   17          TEMP(J)=Y(12)
   18          BRATE(J)=R
   19          RETURN
   20          END


0 MESSAGES FOR ABOVE COMPILATION.

IC VERSION 4 MOD 1
```

SRI TEST PII=269 PROPELLANT PA=165 AR=3.4

INPUT DATA

TO =	25.000	RBAR =	0.330
PA =	15.000	RMIN =	0.001
AR =	8.300	NBAR =	0.400
KN =	238.000	TFBAR=	2910.000
ANR =	3.400	TSBAR=	600.000
TOPFN=	0.001	RHOS =	0.062
LSTAR=	316.000	GAMMA=	1.220
EPS =	1.000	CSTAR=	4500.000

TIME	PPESSURE	DLPDT	RATE	SRATE	TEMPF	TEMPC
0.	518.88	0.0165	0.2514	0.2514	2910.0	2910.0
0.00199	403.86	-190.5751	0.2152	0.2252	2869.0	2786.1
0.00399	284.59	-160.5335	0.1742	0.1919	2823.7	2637.2
0.00599	211.61	-136.7976	0.1456	0.1664	2792.1	2537.9
0.00799	164.05	-118.6995	0.1238	0.1464	2763.3	2474.1
0.00999	131.24	-105.1003	0.1064	0.1303	2735.0	2434.4
0.01199	107.47	-95.2216	0.0919	0.1169	2704.7	2409.4
0.01399	89.49	-88.3008	0.0794	0.1055	2671.5	2392.4
0.01599	75.36	-83.8952	0.0684	0.0954	2633.8	2377.8
0.01799	63.88	-81.7725	0.0584	0.0865	2589.9	2361.3
0.01999	54.26	-81.7417	0.0491	0.0782	2538.1	2339.4
0.02199	46.00	-83.4874	0.0405	0.0704	2477.4	2309.6
0.02399	38.82	-86.3218	0.0327	0.0630	2409.6	2270.8
0.02599	32.57	-89.1532	0.0260	0.0560	2339.3	2223.7
0.02799	27.20	-90.8756	0.0205	0.0495	2273.3	2171.3
0.02999	22.73	-86.5877	0.0163	0.0435	2216.5	2118.2
0.03199	19.40	-69.9306	0.0132	0.0388	2165.7	2072.9
0.03399	17.28	-45.2097	0.0110	0.0356	2114.3	2041.8
0.03599	16.16	-22.7002	0.0094	0.0338	2059.9	2024.5
0.03799	15.67	-9.8257	0.0082	0.0330	2005.6	2014.8
0.03999	15.46	-4.6725	0.0072	0.0327	1956.2	2006.8
0.04199	15.35	-2.7005	0.0065	0.0325	1912.9	1997.8
0.04399	15.28	-1.8715	0.0060	0.0324	1875.2	1987.9
0.04599	15.23	-1.3502	0.0055	0.0323	1842.2	1977.2
0.04799	15.19	-1.0393	0.0051	0.0323	1813.1	1966.1
0.04999	15.17	-0.8360	0.0048	0.0322	1787.0	1954.8
0.05199	15.15	-0.5604	0.0045	0.0322	1763.7	1943.5
0.05399	15.13	-0.5915	0.0042	0.0322	1742.6	1932.4
0.05599	15.12	-0.4264	0.0040	0.0322	1723.4	1921.5
0.05799	15.10	-0.3360	0.0038	0.0321	1705.8	1910.8
0.05999	15.09	-0.2866	0.0036	0.0321	1689.6	1900.4
0.06199	15.09	-0.2629	0.0035	0.0321	1674.6	1890.2
0.06399	15.08	-0.2225	0.0033	0.0321	1660.7	1880.4
0.06599	15.07	-0.2090	0.0032	0.0321	1647.7	1870.8
0.06799	15.07	-0.1810	0.0031	0.0321	1635.6	1861.5
0.06999	15.06	-0.1428	0.0030	0.0321	1624.3	1852.4
0.07199	15.06	-0.1205	0.0029	0.0321	1613.6	1843.7
0.07399	15.05	-0.1011	0.0028	0.0321	1603.5	1835.2
0.07599	15.05	-0.0840	0.0027	0.0320	1594.0	1826.9
0.07799	15.05	-0.0725	0.0026	0.0320	1585.0	1818.9
0.07999	15.05	-0.0488	0.0026	0.0320	1576.4	1811.1

ES = 20.000
EG = 20.000
CSCG = 0.750
FEXT = 0.
ALPHA= 0.000250

TEMPS	TLAST	DEPTH	NOZZLE	EXPONENT
579.95	79.50	0.00257	0.03487	0.4309
568.89	75.66	0.00301	0.11857	0.4457
554.31	70.92	0.00372	0.11857	0.4693
542.34	67.35	0.00445	0.11857	0.4920
531.79	64.46	0.00523	0.11857	0.5134
522.20	62.05	0.00609	0.11857	0.5337
513.14	59.96	0.00705	0.11857	0.5529
504.35	58.12	0.00815	0.11857	0.5712
495.53	56.46	0.00946	0.11857	0.5891
486.39	54.90	0.01108	0.11857	0.6067
476.64	53.41	0.01318	0.11857	0.6244
466.07	51.93	0.01598	0.11857	0.6425
454.68	50.44	0.01979	0.11857	0.6614
442.89	48.93	0.02492	0.11857	0.6809
431.05	47.45	0.03154	0.11857	0.7008
420.05	46.07	0.03961	0.11857	0.7204
410.24	44.88	0.04882	0.11857	0.7374
401.82	43.88	0.05872	0.11857	0.7496
394.73	43.07	0.06885	0.11857	0.7565
388.75	42.40	0.07892	0.11857	0.7597
383.68	41.85	0.08881	0.11857	0.7611
379.29	41.39	0.09848	0.11857	0.7618
375.46	40.98	0.10791	0.11857	0.7623
372.07	40.63	0.11712	0.11857	0.7626
369.04	40.31	0.12611	0.11857	0.7629
366.31	40.03	0.13489	0.11857	0.7630
363.82	39.77	0.14346	0.11857	0.7632
361.55	39.53	0.15185	0.11857	0.7633
359.46	39.31	0.16005	0.11857	0.7634
357.53	39.11	0.16808	0.11857	0.7635
355.73	38.92	0.17594	0.11857	0.7635
354.06	38.75	0.18365	0.11857	0.7636
352.49	38.59	0.19121	0.11857	0.7636
351.02	38.43	0.19862	0.11857	0.7637
349.64	38.29	0.20590	0.11857	0.7637
348.33	38.16	0.21305	0.11857	0.7638
347.09	38.03	0.22008	0.11857	0.7638
345.92	37.91	0.22699	0.11857	0.7638
344.80	37.80	0.23378	0.11857	0.7638
343.74	37.69	0.24047	0.11857	0.7638
342.72	37.59	0.24705	0.11857	0.7639

IX. PRESENTATIONS AND PUBLICATIONS

"Propellant Extinction," Presented at 3rd AFOSR combined Contractor's Meeting, Cocoa Beach, Florida, June 1967.

"Depressurization Induced Extinction of Burning Solid Propellant," by Horton, et.al., AIAA J. 2, 1968.

"Design Considerations for Combustion Stability," presented at ICRPG/AIAA 3rd Solid Propulsion Conference, Atlantic City, New Jersey, June, 1968.

"Design Considerations for Combustion Stability," by R. L. Coates and M. D. Horton, Journal of Spacecraft and Rockets, 6, 1969.

"Extinction of Burning Solid Propellants," Presented at 5th AFOSR Combined Contractor's Meeting, Denver, Colorado, June 1969.

"The Effect of Radiant Energy on the Burning Rate of a Composite Solid Propellant," by M. D. Horton and L. B. Youngberg, submitted to AIAA Journal.

"Prediction of Conditions Leading to Extinguishment," Presented at 6th ICRPG Solid Propellant Combustion Conference, Pasadena, California, October 1969.

UNCLASSIFIED

Security Classification

DOCUMENT CONTROL DATA - R & D

Security classification of title, body of abstract and indexing annotation must be entered when the overall report is classified)

1 ORIGINATING ACTIVITY (Corporate author)	2a. REPORT SECURITY CLASSIFICATION
Brigham Young University Chemical Engineering Science Department Provo, Utah 84601	UNCLASSIFIED 2b. GROUP

3 REPORT TITLE

QUENCHING OF SOLID PROPELLANT COMBUSTION

4 DESCRIPTIVE NOTES *(Type of report and inclusive dates)*

Scientific Final

5 AUTHOR(S) *(First name, middle initial, last name)*

Marvin D Horton
Ralph L Coates

6 REPORT DATE	7a. TOTAL NO. OF PAGES	7b. NO. OF REFS
March 1970	50	16

8a. CONTRACT OR GRANT NO AF-AFOSR-0897-67	9a. ORIGINATOR'S REPORT NUMBER(S)
b. PROJECT NO 9711-01	
c. 61102F	9b. OTHER REPORT NO(S) *(Any other numbers that may be assigned this report)*
d. 681308	AFOSR 70-1376TR

10. DISTRIBUTION STATEMENT

1. This document has been approved for public release and sale; its distribution is unlimited.

11 SUPPLEMENTARY NOTES	12. SPONSORING MILITARY ACTIVITY
TECH, OTHER	AF Office of Scientific Research (SREP) 1400 Wilson Boulevard Arlington, Virginia 22209

13. ABSTRACT

This report presents a transient combustion model and its use in describing the quenching of burning solid propellants. The model combines the transient combustion model of Dennison and Baum with the emperically determined steady state burning rate relationship. Comparison with experiment shows that the model correctly describes the quenching process and also encompasses several effects that were previously unexplained.

DD FORM 1 NOV 65 1473

UNCLASSIFIED

Security Classification

14. KEY WORDS	LINK A		LINK B		LINK C	
	ROLE	WT	ROLE	WT	ROLE	WT
Extinction						
Termination						
Transient solid propellant combustion						
Quenching						